Fall 2016

Spatial Variability of Snow Chemistry of High Altitude Glaciers in the Peruvian Andes

Lindsay K. Wallis
Western Washington University, wallisl@wwu.edu

SPATIAL VARIABILITY OF SNOW CHEMISTRY OF HIGH ALTITUDE GLACIERS IN THE PERUVIAN ANDES

By

Lindsay K. Wallis

Accepted in Partial Completion
of the Requirements for the Degree
Master of Science

Kathleen L. Kitto, Dean of the Graduate School

ADVISORY COMMITTEE

Chair, Dr. Ruth M. Sofield

Dr. Robin A. Matthews

Dr. Carl G. Schmitt

MASTER'S THESIS

In presenting this thesis in partial fulfillment of the requirements for a master's degree at Western Washington University, I grant to Western Washington University the non-exclusive royalty-free right to archive, reproduce, distribute, and display the thesis in any and all forms, including electronic format, via any digital library mechanisms maintained by WWU.

I represent and warrant this is my original work, and does not infringe or violate any rights of others. I warrant that I have obtained written permissions from the owner of any third party copyrighted material included in these files.

I acknowledge that I retain ownership rights to the copyright of this work, including but not limited to the right to use all or part of this work in future works, such as articles or books.

Library users are granted permission for individual, research and non-commercial reproduction of this work for educational purposes only. Any further digital posting of this document requires specific permission from the author.

Any copying or publication of this thesis for commercial purposes, or for financial gain, is not allowed without my written permission.

Lindsay K. Wallis
November 1, 2016

SPATIAL VARIABILITY OF SNOW CHEMISTRY OF HIGH ALTITUDE GLACIERS IN THE PERUVIAN ANDES

A Thesis
Presented to
The Faculty of
Western Washington University

In Partial Fulfillment
Of the Requirements for the Degree
Master of Science

By
Lindsay K. Wallis
November 2016

Abstract

Atmospheric contaminants become incorporated in glaciers through both wet and dry deposition. Some of this particulate matter can act as a source of contamination to glacial streams, leading to a concern for the chemical contamination to cause downstream toxicity to aquatic organisms and toxicity to people ingesting that water. Other portions of this particulate matter, including black carbon, can decrease the amount of light reflected off the snow, thereby contributing to increased rates of glacial melting. These issues are especially of concern to tropical glaciers, which are receding rapidly and are relied on heavily to provide drinking water in the dry season. A snow sampling campaign was conducted on the glaciers of seven mountains in the Cordillera Blanca mountain range in Peru during June-August, 2015 to determine concentrations of inorganic contaminants and black carbon in the upper layer of snow on high altitude glaciers (>5000 m.a.s.l.). Elevation did not appear to be a factor in chemical concentrations, as there were no significant linear relationships with measured analytes and elevation, with the exception of Zn on one mountain sampled. Snow samples on two of the mountains had higher As and Pb concentrations than U.S. Environmental Protection Agency (USEPA) established water quality criteria for human health. Five metals (Al, Cd, Fe, Pb, and Zn) were found to exceed the USEPA aquatic life criteria in at least one sample. The highest concentrations of black carbon and metals were found closest to a local population center and lowest were found in areas furthest from anthropogenic influences. This study also provides supporting evidence that soil/dust is a contributing source of particulate matter but not the light absorbing fraction. An initial attempt at sourcing the particulate matter in these samples was made through an examination of analyte ratios, correlations, and principal components analysis. Multivariate analysis, including hierarchical clustering on principal components, could not explain categories based solely on concentrations of light absorbing particles or distance from the closest large city in the region. The sources of contaminants in the area appears to be complicated, and further studies would provide more insight into the source and spatial distribution of particulate matter on these tropical glaciers.

Keywords: Peru, tropical glaciers, metals, particulate matter, black carbon

Acknowledgments

Many thanks go out to Dr. Ruth Sofield for providing unending guidance and support throughout this process, Dr. Robin Matthews for being an irreplaceable source of knowledge and expertise on multivariate statistical analysis, and Dr. Carl Schmitt for providing the original idea for the project, offering numerous guiding and clarifying comments, and serving as the black carbon analyst and expert.

Muchas gracias a Joaquin y Joel Vargas for their unending help and enthusiasm throughout the expeditions. Special thanks to all the climbers who helped collect and filter samples, including Dr. John All, Dr. Rebecca Cole, Meg Harris, Jordi Johnson, Roberto Noensie, Alec Pankow, Wilmer Rodriguez, Chandler Santos, Dr. Carl Schmitt, Michael Solomon, Robin Thomas, and Alex Young. Extra thanks to Robin Thomas for helping with GIS. Many thanks to Ed Bain, Dan Carnevale, Ariana Dionisio, Erin Macri, Kyle Mikkelsen, and Charles Wandler (Western Washington University [WWU]) for their help with analytical instrumentation. Extra thanks to Ed Bain for providing encouragement and background knowledge for this project.

This study was graciously made possible with funding support from the American Climber Science Program, The Explorer's Club, WWU Dean's Sustainability Fund, and Huxley College Small Grants.

Table of Contents

List of Tables

List of Figures

List of Supplementary Information

1. Introduction

1.1 Overview

1.1.1 General overview

Snow chemistry of glaciers is worth examining for three main reasons: 1) snow chemistry can act as a marker for atmospheric chemistry because of atmospheric deposition onto snow; 2) contaminants in the snow can be a source of contamination to glacial streams, leading to a concern for downstream toxicity to aquatic organisms and people ingesting that water; and 3) particulate matter, especially black carbon, can decreases the amount of light reflected off the snow, thereby contributing to increased rates of glacial melting. This final effect will be particularly important in the tropical glaciers, which experience higher intensity solar irradiation and will experience greater increases in ambient air temperatures than mid- and high latitude glaciers (MRI 2015). The largest concentration of tropical glaciers in the world is in the Cordillera Blanca (White Mountains) in Peru (Kaser et al. 1990). My study examined issues relating to snow chemistry in the Cordillera Blanca mountain range.

1.1.2 Terminology

Because of the interdisciplinary nature of this work, terminology is important to clarify. In this thesis, "particulate matter" or "particulates" refers to the total solids found in and on the glaciers. The term "black carbon" refers to the carbon fraction of the particulate matter that absorbs light. Black carbon is sometimes used synonymously with "soot", which is specifically referring to the formation process of these particulates. Thus, "soot" is a formation/source designation, while "black carbon" is an optical and chemical designation. "Light absorbing particles" is an optical designation that refers to black carbon and any other total solids that contributes to the light absorption, regardless of their origin or chemical composition. The

specific technique used for my analysis used an optical process to quantify light absorbing particles and resulted in values of "effective black carbon" (eBC). All contaminants that were measured in my study were referred to as "analytes" and those measured through chemical techniques (metals and inorganic anions) were referred to as "chemical analytes".

1.1.3 Study area

The Andes hold 99% of the world's tropical glaciers, with Peru alone hosting 70% (Kaser and George 1999, Mark et al. 2010). Approximately one-quarter of all the tropical glaciers in the world are contained within the Cordillera Blanca (Vuille et al. 2008); however, these glaciers have been receding rapidly, with a total loss of over 30% from the 1930's to present (Schauwecker et al. 2014) and an estimated loss of 20% from 1970-2003 (Racoviteanu et al. 2008). The implications on water discharge as a result of glacial recession are still to be determined, but could result in decreased discharge during the dry season (Pouyaud et al. 2005, Baraer et al. 2012), a change in the seasonality of discharge but not the total volume of discharge (Juen et al. 2007, Vuille et al. 2008), or a decrease in the total amount of discharge (Mark et al. 2005, Mark et al. 2010, Baraer et al. 2012). Regardless of the exact change, there could be large implications to the estimated 50 million individuals in the Andean valleys that rely on these glaciers for drinking water, agriculture, and hydroelectricity (Nagy et al. 2006, Stern 2008).

1.2 Background

1.2.1 Atmospheric deposition

The chemical composition of high altitude glaciers is highly variable due to the changing composition of both wet and dry atmospheric deposition onto glaciers. Wet deposition occurs when chemicals or particles are incorporated into or on precipitation where they are deposited

on the snow, while dry deposition (i.e. sedimentation) occurs through the direct deposition from the atmosphere to snow, without the incorporation of precipitation (Kuhn et al. 2001, Larose et al. 2013). Thus, snow chemistry is a product of both wet and dry deposition and can be a good tool for the evaluation of atmospheric transport and deposition of these contaminants (Walker et al. 2003, Gabrielli et al. 2006). However, interpretation is further complicated by the fact that chemicals have the ability to move and change after being deposited on glaciers, leading to a complicated and dynamic system (Davies et al. 1987, Scotterer et al. 2003).

Because trace metals are ubiquitous in use and release and have been found to be a constituent of the atmosphere, even in remote locations (Marx et al. 2014), determining their source can be difficult. However, specific chemical analytes are found more commonly as the result of particular types of release, so identifying those can help suggest a probable source. The largest global source to the atmosphere of Cr, Hg, Mn, Sb, Se, Sn, and Tl is coal combustion, of Ni and V is oil combustion, of Pb is gasoline combustion, and of As, Cd, Cu, In, and Zn is hard-rock mining (Pacyna and Pacyna 2001). But there are other sources (both natural and anthropogenic) for those and other metals, and none of the metals listed above are unique to the single, listed source. For example, other contaminants released from gasoline combustion in vehicles are NO_3, As, K (Almeida et al. 2006), Pb, Zn (Song et al. 2006), and SO_4 (de Caritat et al. 2005). Sourcing contaminants is therefore a complicated process, but the identification of certain chemicals and their relationships can lead to a better understanding of where the contaminants originated.

Expected local contaminant sources in the Cordillera Blanca include anthropogenic release from oil and gasoline combustion (primarily from vehicles, residential heating and cooking, and industrial pollution), especially from Huaraz, the closest large (approximately 100,000 people) population center to the Cordillera Blanca. An additional local contaminant

source may be the two hard-rock mines located near the Cordillera Blanca. The Pierina Mine is a Au and Ag open-pit mine located 10 km north of Huaraz and the Antamina Mine is a Cu and Zn mine located in the Cordillera Occidental, 50 km east of Huaraz on the largest known Cu-Zn ore deposit that also contains Mo and Ag (Love et al. 2004). The mining industry has been identified as a large local contributor of black carbon in some areas of the world, mainly through diesel emissions (Evans et al. 2015). An additional local source of contaminants may come from biomass burning, as forest fires can be prevalent at certain times of the year and agricultural burning is a common occurrence (Molina et al. 2015). Biomass burning has been found to be a contributor of K and Cl (Watson and Chow 2001), black carbon, and organic ions such as oxalate, formate, and levoglucosan (Hegg et al. 2009).

An additional question about atmospheric deposition is what influence elevation has on snow chemistry. Due in part to the role of orographic precipitation, elevation-dependent deposition patterns would be expected. This phenomenon of increasing concentrations of contaminants with increasing elevation has been seen in some studies (Dore et al. 1992, Lovett and Kinsman 1990), but not in others (Kang et al. 2007) and this relationship in the Cordillera Blanca has not been established.

1.2.2 Influence of light absorbing particles on albedo

The presence of light absorbing particles on the snowpack reduces the albedo, or whiteness, of the snow, which can decrease its reflective properties and warm the snowpack surface (Warren and Wiscombe 1980a, Warren and Wiscombe 1980b, Warren 1984, Bond et al. 2013). Through this mechanism, light absorbing particles have the potential to increase the rate of glacial recession through increased snow melting and influence the hydrology of certain areas (Hansen and Nazarenko 2004, Hadley et al. 2010). The main anthropogenic contributor of the decreased

albedo is black carbon, which acts as an efficient absorber of visible light and solar radiation, making it a key player in global climate change (Bond et al. 2007, Kopp and Mauzerall 2010). The largest worldwide contributor of black carbon is the burning of biomass, including wildfires and agricultural burning (USEPA 2011), and these activities have been shown to be the largest source of black carbon deposited in snowpack in different areas across the globe (Hegg et al. 2009). The second largest contributor is residential heating and cooking, while industry and motorized transportation contribute most of the rest, with a small percentage coming from other miscellaneous sources (Hegg et al. 2009).

Even low concentrations of light absorbing particles (2-30 ng/g) have been shown to lead to a decrease in surface albedo depending on other factors such as snow grain size and solar angle (Warren and Wiscombe 1985). A decrease in albedo has been shown to have direct effects on snow cover in numerous studies. The addition of dark particulates on glaciers has been identified as a possible cause of glacial recession in the Himalayas (Menon et al. 2010). Dark particles have been attributed with causing a decrease in up to 10 days less of snow cover in areas of North America and Eurasia (Ménégoz et al. 2013, 2014), the end of the Little Ice Age (Painter et al. 2013), and glacial recession in the Andes (Molina et al. 2015). These impacts underscore the importance of understanding black carbon extent to better predict potential effects.

1.2.3 Glacial melt toxicity

In addition to the potential to impact water quantity, contaminants on glaciers can also influence water quality. It is estimated that there are currently one billion people worldwide who rely on glaciers for a source of freshwater, and this number is expected to reach 1.5 billion by 2050 (Barnet et al. 2005). The exact contribution of glaciers to meltwater volume varies greatly

depending on a variety of factors, but it is estimated that some tropical glaciers contribute approximately 40% of the total water in downstream glacial streams, with much higher contributions possible during the dry season (Mark and Seltzer 2003). Laboratory and field studies have shown that the first meltwater fractions contain higher concentrations of contaminants (up to five times higher) than the bulk snowpack, through a process called ionic pulse (Johannessen et al. 1976, Colbeck 1981). This rapid release of ions (particularly H and Al) can decrease the pH of surrounding waters. This episodic acidification has the potential to cause toxic effects to organisms both directly (through low pH waters) and indirectly by increasing the solubility of toxic metals (Wright et al. 1976, Johannessen and Henriksen 1978, Tranter et al. 1987, Wigington et al. 1990). In addition, accumulated contaminants in glaciers have the potential to cause downstream effects through direct toxicity when released during melting. However, the toxicity potential of metals in glacial streams can be decreased through a variety of natural attenuation processes such as dilution, decreased solubility, or sorption to organic matter (Webster et al. 1994, Gangy et al. 2007). Thus, the identification of toxicity potential of glacial waters does not necessarily imply downstream toxicity, which is reliant on numerous water chemistry and hydrology parameters.

1.3 Study objectives

The goals of my project were: 1) to evaluate atmospheric deposition patterns in the area by examining the spatial distribution of light absorbing particles and other contaminants in and on the glaciers, including elevation and proximity to a population center; 2) to attempt to determine sources of these contaminants through a variety of statistical analyses, including pairwise comparisons of sites classified by their distance from a population center, correlation analyses, examination of analyte ratios in each samples, principal components analysis, and hierarchical

clustering on principal components using measured contaminant concentrations; 3) to determine toxicological implications of the snow chemistry by examining total vs. dissolved metals and comparing snow chemistry to various water quality criteria.

2. Materials and Methods

2.1 Snow sampling

Snow samples were collected from within the Cordillera Blanca mountain range in west central Peru (Figure 1) by members of the American Climber Science Program during their 2015 expedition (climberscience.org). The Cordillera Blanca mountain range is an area almost entirely encompassed within the Huáscarán National Park, with over 700 glaciers, is home to the largest concentration of tropical glaciers on the planet (Kaser et al. 1990, Mark et al. 2010). Snow samples were collected during this region's dry season (June-August 2015). Within the Cordillera Blanca, snow samples were collected from seven mountains (Alpamayo, Ishinca, Pisco, Tocllaraju, Urus Este, Vallunaraju, and Yannapacha, ranging from 5050 to 5735 m.a.s.l. (Table 1). An attempt was made to sample from multiple elevations on each mountain, with the lowest elevation collected at least 100 m onto the toe of the glacier and at regular intervals (~500 vertical m) along the climbing route on the way to the summit. At each sample location, snow samples were collected from the surface (<~3 cm) to provide a look at the newest snow and for consistency with previous studies. Samples were collected with a plastic scoop and placed into a clean, food-grade polyethylene plastic bag where they were transported to basecamp and prepared for further analysis.

2.2 Sample analysis

2.2.1 Light absorbing particles

Snow samples were rapidly melted by placing the bags in hot water, then 600 mL of melted snow were pumped through 0.7 μm quartz fiber filters (type 25 mm; Pallflex Tissuquartz; Pall Corporation) using clean plastic syringes. The filters were dried and stored, then shipped to Colorado, USA to determine concentrations of light absorbing particles (in units of effective black carbon [eBC]). This was determined by Dr. Carl Schmitt using the Light Absorption Heating Method (LAHM) in the same manner as Schmitt et al. (2015).

2.2.2 Metals and inorganic anions

Aliquots from the melted snow samples described in Section 2.2.1 were subdivided into 15 mL plastic vials to determine total (unfiltered) and dissolved (snow filtered through 0.45 μm PVDF filters [Fisherbrand]) metals. The aliquots were acidified to 2% with metal-grade nitric acid before analysis at Western Washington University (WWU), USA. Additionally, unacidifed, 0.45 μm PVDF filtered, melted snow was stored in 2 mL plastic centrifuge vials for anion concentration analysis. Chemical analytes included metals (Be, Na, Mg, Al, K, Ca, V, Cr, Mn, Fe, Co, Ni, Cu, Zn, As, Se, Mo, Ag, Cd, Sb, Ba, Tl, Pb, Th, and U) and inorganic anions (F, Cl, NO_3, and SO_4), which were analyzed by Ed Bain (WWU) and Charles Wandler (Scientific Technical Services, WWU), respectively. Metals were analyzed with inductively coupled plasma mass spectrometry (ICP-MS; Agilent 7500ce) with added octopole reaction system for ion interference removal. Anion determination was performed with high performance liquid chromatography (Varian 240 ProStar) with a 4 x 250 mm analytical column (Dionex Ion Pac AS14A) and 4 x 50 mm guard column (Dionex Ion Pac AS14G) with an 8 mM Na_2CO_3/1 mM $NaHCO_3$ eluent (1.0

mL/min flow rate), Dionex AMMS 300 suppressor (50 mN H_2SO_4 at approximately 3 mL/min flow rate), and Waters 432 ion detector.

2.3 Statistical analysis

2.3.1 Descriptive statistics

All statistical analyses were calculated using RStudio (R Core Team 2016). Many of the variables did not meet parametric assumptions of normality and homoscedasticity, so nonparametric, rank based tests were used when possible. Pairwise comparisons were performed with the Kruskal-Wallis Rank-Sum test, with an alpha of 0.05. Correlations were determined using Kendall's Ranked Correlation test. Where there were multiple isotopes of an analyzed element, the most common isotope was chosen for statistical analyses (e.g.^{52}Cr, not ^{53}Cr; ^{107}Ag, not ^{109}Ag) to avoid redundancy. For each sample, the summed total metal concentration was determined by taking the sum of concentrations of each of the total (unfiltered) metals and used for statistical classification, with "High" metals being those with concentrations higher than the median total metal concentrations and "Low" metals equal to those below.

2.3.2 Spatial analysis

ArcGIS (Esri 2015) was used to create maps (with the assistance of Robin Thomas, WWU), calculate distances with the point distance tool, and estimate aspect with the hillshade layer. For statistical analysis, samples were grouped as: a) all mountains and all elevations (referred to as "Combined samples"); b) all mountains and elevations near or all mountains and elevations far (referred to as "Near samples" and "Far samples", respectively); and c) all elevations from a mountain (referred to by the specific mountain name). Samples were categorized into Near

samples or Far samples based on a natural break in the distances from sample locations to Huaraz, Peru (Figure 1).

2.3.3 Exploratory data analysis

Mass ratios of chemical analytes at each sample location were calculated to attempt source determination. This consisted of ratios of Na/Cl, SO_4/Cl, and NO_3/SO_4. The Na/Cl ratio was determined at each site to determine the derivation from normal sea salt ratios (0.56 on a mass basis [Möller 1990]). The Cl/SO_4 ratio at each sample was compared to the typical ratio of 7.1 in seawater (Kroopnick 1977). The ratio of SO_4/NO_3 was examined to determine if stationary emissions were more dominant (Wang et al. 2005).

Exploratory data analysis using various multivariate statistical techniques was used to identify relationships and patterns within the data. For all multivariate statistical analysis, total metals were chosen over dissolved metals to avoid including redundant variables. Total metals were selected because they provide higher concentrations and limit the number of samples at or below detection limits. All analytes that had more than half of the samples below the detection limit were removed from multivariate analysis. Principal component analysis was performed on scaled, centered variables, followed by hierarchical clustering on principal components using Euclidean distance with Ward's method to retain groups with small internal variance. Post hoc testing was done using Pearson's Chi-squared test with Yates' continuity correction to determine if program-determined clusters (from "cutree" in R) matched with hypothesized groups. Another method of clustering was performed with the RIFFLE.R package, a nonparametric and nonmetric clustering tool (Matthews and Hearn 1991, Matthews and Matthews 2006). This method of clustering does not use a distance metric when analyzing variables, making it ideal for a non-normal dataset. The proportional reduction in error terms (PRE values) were obtained for

multiple trials to determine the variables to cluster on and the derivation from random chance for cluster association.

3. Results and Discussion

3.1 Spatial distribution

3.1.1 Proximity to Huaraz

Higher eBC values and many of the individual metals were found closer to Huaraz, as indicated by both a significant correlation between variables and significant results with the Kruskal-Wallis pairwise testing on Near samples compared to Far samples (Figure S1, Table 2).

There were higher concentrations of the summed total metals in the Near samples compared to Far samples ($p<0.05$, Kruskal-Wallis; Figure 2). Only some of the individual analytes (eBC, SO_4, Ca, Mn, Pb, and As) were significantly higher in the Near samples compared to Far samples ($p<0.05$, Kruskal-Wallis, Table 2). Collectively however, most of the median concentrations (with the exception of Cr), were higher in Near samples compared to Far samples (Table 2). The higher eBC values in the Near samples provides some evidence that eBC may be originating from or near Huaraz. This is further evidenced by the higher presence of SO_4, Pb, and As in the Near samples, which are all markers of anthropogenic influences, especially related to vehicle exhaust/fuel combustion/traffic (Almeida et al. 2006, de Caritat et al. 2005). However, other markers of vehicle exhaust and fuel combustion (NO_3, Cu, and Zn) do not show significant differences in concentrations in Near and Far samples. Additionally, Pb and As may have an additional local source, as they are naturally occurring in local rocks (Bodenlos and Ericksen 1955, Lipten and Smith 2005). Therefore, the higher concentrations of Pb and As in the Near samples may also be the result of those samples being nearer to hard-rock mining operations or other processes that may release these metals or having different local geology

than the Far samples. Additionally, other differences between Near and Far samples (besides proximity to Huaraz) may be driving the differences seen between these samples, including latitude, location on the mountain range, and ability for atmospheric transport.

3.1.2 Influence of elevation

There was no significant linear relationship between elevation and any of the measured analytes for Combined samples (Figure 3) or on each of the mountains individually (Figures S2-S5). The only exception to this was a significant increase in Zn with increasing elevation on Ishinca ($p<0.05$; Figure S2); however, given the large number of analytes measured and tested, it is not surprising to have at least one analyte showing a statistically significant relationship using an alpha of 0.05 (Type I error). A limitation of these data is that these results are from only three or four samples at different elevations on each mountain, with no replicates at an elevation.

There were no significant correlations ($p>0.05$) with elevation and any measured analytes for the Combined samples or Far samples. The Near samples had significant, positive correlations with elevation and V, Fe, Mg, and Al ($\tau=0.86$), Co ($\tau=0.71$) and Mo ($\tau=0.64$). The full lists of correlation coefficients with analytes and elevation are shown in Tables S1-S3.

3.1.3 Comparison to other surface albedo studies

In my snow samples, eBC values ranged from 4.7 to 170 ng/g, with the samples nearest to Huaraz ranging from 34-170 ng/g and more remote samples ranging from 4.7-110 ng/g. Previous studies that used the same methodology in the same mountain range found eBC values on glaciers in the Cordillera Blanca in Peru to be 20-80 ng/g for the glaciers closest to Huaraz, with the more remote samples in the range of 2-20 ng/g from 2011-2013 (Schmitt et al. 2015). Higher concentrations in 2015 may be in part due to different weather patterns, namely due to

an El Niño year, which could be moving increased levels of pollution from larger cities onto the glaciers (C. Schmitt, personal communication). The lowest value found in my study (4.7 ng/g) is comparable to measurements found using a different method of determination of light absorbing particles, which produced values as low as 2-3 ng/g in Greenland ice sheets and 5-15 ng/g in other areas of the arctic (Grenfell et al. 2009). The highest eBC value found in my study (170 ng/g) was lower than the highest concentrations (greater than 1000 ng/g) found in the northeastern areas of China (Huang et al. 2011). The median values in my study (55 ng/g) were also similar to measurements taken in North America, with values of 22-59 ng/g in Washington, USA (Grenfell et al. 1981) and ~5–70 ng/g across the United States (Pacific Northwest, Northwest Intermountain, and Great Plains) and Canada (Interior Plains and Western Cordillera), with some samples exceeding 100 ng/g (Doherty et al. 2013).

3.2 Source determination

3.2.1 Correlations

There were many significant positive correlations between measured variables in the Combined samples (Table S1). The strongest correlations between variables were between Al, Fe, Mg, and V ($\tau > 0.9$, Tables 3 and S1). This is potentially explained by a strong geochemical influence, because Al, Fe, and Mg are elements commonly used as soil markers in source determination studies (Watson and Chow 2001, Almeida et al. 2006, Song et al. 2006). In addition, V is a common constituent of soil (ATSDR 2012) found in Peruvian metal ore deposits (Bodenlos and Ericksen 1955), despite not being universally considered a soil marker. However, Al and Mg are not a major constituent of the local geology (Bodenlos and Ericksen 1955), leading to uncertainty in treating those elements as soil markers. While these metals had strong correlations with each other, there was a notable lack of significant correlations between eBC and these

metals, especially in Near samples. The correlation coefficients of eBC and the soil marker metals were all less than 0.1 for all but Ca ($\tau < 0.4$). The Far samples had higher correlation coefficients between eBC and these metals ($\tau \leq 0.5$), but the only significant correlation ($p<0.05$) between these metals and eBC was with eBC and Al. The metals had strong, significant correlations with one another ($\tau < 0.8$, $p<0.05$). This presence of soil markers in snow, but lack of relationship with the light absorbing particles, provides evidence that, while soil/dust may be contributing to the contaminant load on the snow (especially for the Far samples), it is not a large source of light absorbing particles. This finding is not surprising given that the method for eBC determination does not distinguish between black carbon and dust (Schmitt et al. 2015).

Although V is a constituent of soil/dust, it is more commonly indicative of fuel combustion. Other common markers of fuel combustion include NO_3, SO_4, K, Zn, Ni, Pb, Cu, As, and Sb [Almeida et al. 2006, Song et al. 2006, de Caritat et al. 2005]). These parameters showed mostly significant, moderate to strong correlations with each other (Table 4), suggesting that fuel combustion may be a contributing source of particulate matter on these glaciers.

There was a significant correlation between Na and Cl for the Combined samples, Near samples, and Far samples (Table 5). None of the common marine biomarkers (Cl, SO_4, Na, and Mg [Wang et al. 2015, Almeida et al. 2006]) were found to be significantly correlated with eBC for either Near or Far samples, but they were correlated with the Combined samples (Table 5). The only significant correlation of marine markers in Far samples was between Na and Cl ($\tau = 0.79$, $p<0.05$). In addition to being further from population centers, the Far samples were also taken at locations that were farther north and tended to be on the eastern (non-ocean) side of the mountain range (Figure 1), which may, at least in part, explain the lack of sea salt correlations. The fact that other differences exist between Near and Far samples in addition to

proximity to population centers is difficult to quantify but important to consider when examining and interpreting results.

There were differences in the relative correlations of Near samples compared to Far samples, as seen in the full correlation coefficient tables for both (Table S2 and S3) and explained in Section 3.1.3. There were no significant correlations with light absorbing particles and any of the measured chemical analytes in Near samples (Table S2). There were significant correlations with eBC and Al, V, As, Sb, and Ba ($\tau = 0.64$; Table S3) for Far samples.

3.2.2 Analyte and eBC relationships

The eBC values were grouped into two categories: "Low eBC" (eBC < 50 ng/g) and "High eBC" (eBC > 50 ng/g), due to greater uncertainty of eBC values above 50 ng/g (C. Schmitt, personal communication) and the eBC sample median of 58 ng/g. The median analyte concentrations for High and Low eBC categories are listed in Table 6. High eBC samples had significantly higher concentrations of Mg, Al, Ca, Mn, Fe, Zn, As, Ba, and Pb compared to Low eBC samples. There were no statistically significant differences in concentrations of Na, K, Cr, Ni, or Cu between High eBC and Low eBC samples. There was a significant positive correlation between the summed total metal concentrations and eBC values ($p<0.01$).

3.2.3 Analyte ratios

The ratios of Na/Cl, Cl/SO_4, and SO_4/NO_3 were used to determine if influences were predominately anthropogenic or nonanthropogenic. The ratio of Na/Cl was less than 0.56 (the typical mass ratio found in seawater) for all but one sample. This suggests that the contaminants measured in the snow were not sourced from the sea and/or there is an additional Cl input to these glaciers. The additional Cl may originate from industrial sources (deCaritat et al. 2005,

Wang et al. 2015), vehicles or coal combustion (Al-Khashman 2009, Xu and Han 2009, Wang et al. 2015), or biomass burning (Watson and Chow 2001). There was a statistically significant difference in the Na/Cl ratios in Near and Far samples ($p<0.05$, Kruskal-Wallis; Figure 4) but no significant linear relationship between distance from Huaraz and Na/Cl ratio ($p>0.05$; Figure 4). This indicates that an anthropogenic process in or near Huaraz may be a source for Cl. Interestingly, the Cordillera Blanca itself is composed of high concentrations of Na (Petford and Atherton 1996) which may present itself in the snow through dust deposition, leading to even stronger evidence for increased Cl loadings from anthropogenic origins.

The Cl/SO_4 ratio ranged from 0.704 to 16.7 in my samples (Figure 5). The typical seawater ratio is 7.1 (Kroopnick 1977). There was no significant difference in the Cl/SO_4 ratios in Near and Far samples ($p>0.05$, Kruskal-Wallis; Figure 5). SO_4 and Cl were found to be significantly correlated with each other for Combined samples (Table S1) and Near samples (Table S2), but not for Far samples (Table S3).

Ratios of SO_4/NO_3 ranged from 1.5 to 7.9 in my samples. Typically, high SO_4/NO_3 ratios are associated with anthropogenic emissions (Wang et al. 2015). There was a significant difference in the SO_4/NO_3 ratios in Near and Far samples ($p<0.05$, Krukal-Wallis; Figure 6), but this difference appeared to be largely driven by two outliers (U2 and T1; Table 1) that have high ratios due to high SO_4 concentrations. There was no significant linear relationship between distance from Huraz and the SO_4/NO_3 ratios ($p<0.05$; Figure 6). There was a significant correlation between SO_4 and NO_3 for Combined samples (Table 4a) and Far samples (Table 4c) but not with the Near samples (Table 4b), which may suggest multiple sources of these chemical analytes for Near samples. Further differences in samples identified with the SO_4/NO_3 ratios is discussed in Section 3.2.4.

3.2.4 Multivariate statistical analysis

Principal components analysis found that the first principal component (PC1) accounted for 56% of the variance, PC2 accounted for 16%, and PC3 accounted for 9.5%. The first three PCs were used for hierarchical clustering due to the stability of clusters (Figure S6). The full variable loadings for the first five PCs are shown in Table 7. The first principal component loaded positively on all variables, indicating that the presence of one analyte generally corresponded with presence of all the rest. This is further evidenced by the presence of large numbers of positive correlations between variables (Table S1). The highest loadings of PC1 came from Ba, K, Mn, and Co, with the largest separation occurring between these variables and Cl, Cr, Cd, and Ni (Table 7). The second principal component showed good positive/negative separation, with NO_3 and Cr showing the highest loading and greatest separation with Cl, Zn, and SO_4.

Hierarchical clustering on principal components separated the samples into two distinct, nonrandom clusters that corresponded with a group composed of Near samples plus one of the Far samples (G2) and a group composed of both Near and Far samples (G1), as shown in Figure 7. The one Far sample (P2) in G2 had concentrations of many chemical analytes closer to the median concentrations found in G2 (Table 8), and higher concentrations of many analytes (F, Cl, NO_3, SO_4, Na, Mg, Al, K, Ca, V, Mn, Fe, Ni, Cu, Zn, As, Mo, Ba, Pb, and U) than the other Far samples. The distinction between P2 from the other Far samples can also be seen in the ordination of principal components (Figure 8).

Only some of the measured analytes were significantly higher in the Near samples than Far samples when looked at individually (Table 2). Collectively however, all but one of the medians were higher in the Near samples than Far samples (Table 8), which formed the basis for

the multivariate analysis. When P2, the lone Far sample in G2, was removed from the analysis, there were significantly higher concentrations of analytes at the Near samples compared to Far samples for all analytes but Cd, Cu, Cr, NO_3, and Na (Table S2).

The two groups, G1 and G2, did not differentiate significantly based on eBC values or distance from Huaraz ($p>0.05$, Pearson's Chi-squared test with Yates' continuity correction). Differentiation based on G1 and G2, and the relationship between Near and Far samples, were also seen when plotted against each other on SO_4 and NO_3, as shown in Figure 9.

With RIFFLE clustering, a nonsignificant association was found with the two groups (RIFFLE 1 and RIFFLE 2) and both eBC and distance categories ($p>0.05$, Pearson's Chi-squared test with Yates' continuity correction; Figure 10). PRE values were obtained for three different trials and, while they changed depending on the trial, Na and K had consistently higher PRE values and were used to plot clusters and groups (Figure 10).

3.3 Toxicological implications

3.3.1 Total vs. dissolved metals

The distinction between total and dissolved metals has implications for the fate and transport, and thus toxic potential, of metals. There were strong, significant correlations seen between total and dissolved metals for the majority of metals analyzed (Table 9). Of those total and dissolved metals that were not significantly correlated with each other (Al, V, Cr, Co, Se, and Cd), low concentrations near the detection limit was a likely explanation with the exception of Al because the concentrations of both total and dissolved Al were well above the detection limits (Figure 11). The solubility of Al in snow is a complicated process that is influenced by a number of factors, including pH, which ultimately influences the dissolved/particulate speciation of Al

(Losno et al. 1993). Measuring the pH of snow samples might shed more light into this lack of correlation between total and dissolved fractions.

3.3.2 Comparison to water quality thresholds

To determine the potential for toxicity of snowmelt to aquatic life, chemical analyte concentrations in all snow samples were compared to freshwater guidelines. The Criterion Continuous Concentrations (CCCs) and Criteria Maximum Concentrations (CMCs) were established by the United States Environmental Protection Agency (USEPA) to minimize risk to the majority of aquatic species present with chronic and acute exposures, respectively (USEPA 2016). The CMCs were determined by the USEPA through an examination of data relating to the contaminant's acute toxicity to animals; CCCs were determined by the USEPA with an examination of data relating to chronic toxicity to animals, toxicity to plants, bioaccumulation potential, and other data (Stephan et al. 1985). The use of the two criteria values was deemed superior to a single value to "more accurately reflect toxicological and practical realities" (Stephan et al. 1985).

All samples but those from Alpamayo had concentrations of Al higher than the Al CCC (0.087 mg/L in waters with a pH of 6.5-9.0) and six samples (I1, I2, I3, V1, V2, and P2; Table 1) had concentrations above the CMC (0.75 mg/L in waters with a pH of 6.5-9.0) for Al. Those same six samples were also above the CCC for Fe (1 mg/L). There is no established CMC for Fe. Two samples (Y1 and P2; Table 1) were above the Cd CCC (0.00072 mg/L) but below the CMC (0.0018 mg/L); all other samples were below both criteria. Nine samples (I1, I2, I3, U1, U2, T1, Y1, P2, V1, and V2; Table 1) were above the Pb CCC (0.0025 mg/L). Two samples (T1 and U2; Table 1) were above the CMC and CCC of 0.120 mg/L for Zn. All other samples had

analyte concentrations below the established CMCs and CCCs. It should be noted that the CCC/CMC established for Al is based on a limited number of studies and has relative uncertainty associated with pH and water hardness dependent solubility issues (USEPA 1988).

Chemical analyte concentrations were also compared to human health criteria to determine the toxic potential of meltwater. The USEPA determines maximum contaminant levels (MCLs) as legally enforceable maximum concentrations of contaminants in waters that will be used as public drinking water, as determined by health-based data with margins of safety (USEPA 2016). Two samples on Ishinca (I1 and I3; Table 1) had concentrations of Pb and As higher than the MCLs of 0.015 mg/L and 0.010 mg/L respectively (USEPA 2009). One sample (V1; Table 1) was also above the USEPA MCL for Pb (USEPA 2009). All other samples were below USEPA MCLs for all measured chemical analytes.

4. Conclusions and future directions

4.1 Spatial

Concentrations of light absorbing particles were found to be similar to other studies across the globe, with levels higher than in previous years in the Cordillera Blanca mountains. The lowest eBC values were found in the glaciers farthest from human population centers and were comparable to remote Arctic measurements. The highest eBC values were closest to the largest city in the region and were comparable to North America and Asia measurements, but less than the highest measurements found globally. Even the lowest values of eBC found in my study (5 ng/g) have been shown to lead to a decrease in surface albedo (Warren and Wiscombe 1985). Thus, the amounts of light absorbing particles on the glaciers of the Cordillera Blanca, even at the lowest concentrations in my study, have the potential to decrease surface albedo, increase snow melting, and contribute to glacial recession.

Differences in snow chemistry do not appear to be explained by elevation, as there were no statistically significant patterns associated with increasing elevation. However, the limited number of samples and replicates on each mountain makes it difficult to evaluate the influence of elevation with any certainty. A more extensive sampling effort might provide clarity.

4.2 Source

Differences were found between Near and Far samples that provides weak evidence that the population center of Huaraz may be contributing contaminants to the glaciers of the Cordillera Blanca. There were significantly higher eBC values and concentrations of certain contaminants at the sites nearest to Huaraz, chemical concentrations had different relationships for Near samples vs. Far samples, and the high Cl concentrations, low Na/Cl ratios, and high SO_4/NO_3 ratios, especially in the Near samples, are indicative of an anthropogenic contribution of contaminants to the glaciers. However, the differences in the Near vs. Far samples may not be solely driven by the city itself, as there are other differences between the sites themselves. For instance, both latitude and the location of the mountain within the Cordillera Blanca could influence the deposition patterns of contaminants. Additionally, differences in clustering were found to be at least partially explained by snow chemistry but involves more than just proximity to population centers in determining the amounts of chemical concentrations on the glaciers.

My study found evidence that eBC is not explained by dust, as there was a lack of correlation with soil analyte markers with eBC values. This, and the fact that there was a high correlation between the soil analytes themselves, suggested that dust is present on the glaciers but not contributing to decreased albedo on the glaciers.

For more definitive source determination, more specific markers would need to be quantified. Different organic compounds, such as vanillin, levoglucosan, oxalate, and formate all

act as proxies for biomass burning and their presence would help determine the contribution of biomass burning to contaminants on the glaciers (Hegg et al. 2009). Additionally, larger numbers of samples would allow for source determination software (like the USEPA's Positive Matrix Factorization [Hegg et al. 2009]) to be utilized, providing higher confidence in source determination.

4.3 Toxicological

Snow samples that were higher than established freshwater criteria for human and aquatic life were identified. These guidelines were established for surface water, not snow, but the contaminant concentrations in the snow may ultimately affect water quality downstream when the snow melts and water (and metals) travel into glacial lakes and streams. Because meltwater from these glaciers moves to glacial streams and ultimately drinking water for local communities, concentrations of potentially toxic metals above criterion warrant further investigation, including a more detailed examination of how the meltwater chemistry changes from source to sink, and how this changes throughout the seasons.

Additionally, a more in depth examination of the role that chemical speciation (ex. inorganic vs. organic arsenic) plays in glacial systems would be helpful in determining the toxic potential of metals to aquatic organisms in this system. Further, a study including contaminants known to be persistent (ex. PAHs, PCBs, etc.) would give a more comprehensive understanding of the toxic potential of glacial meltwater. However, a full toxicological study would also need to address natural attenuation processes, including sorption, dilution, and solubility, that could decrease the toxicity of glacial melt water downstream.

Figures

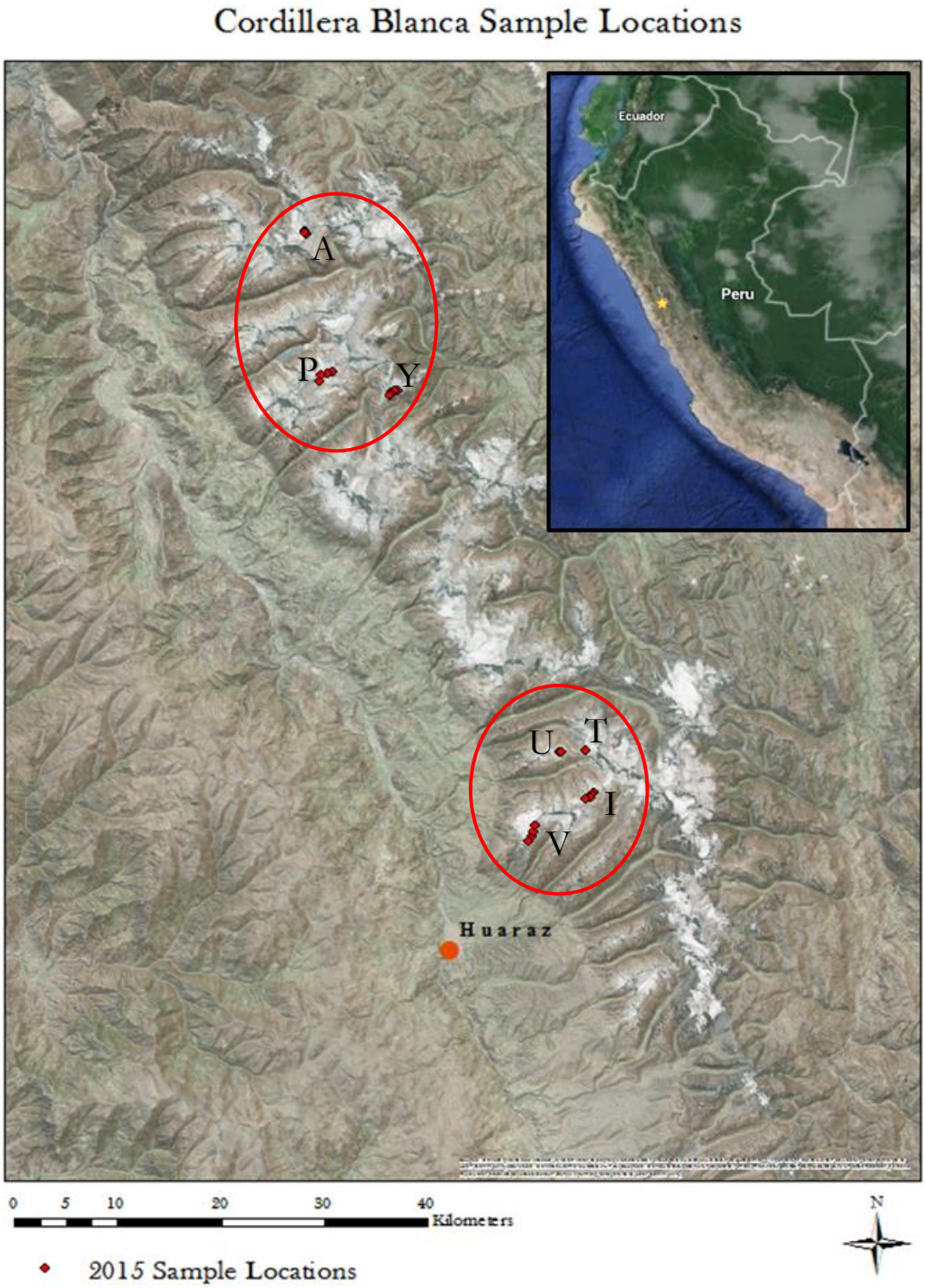

Figure 1. Map of Cordillera Blanca snow sampling locations in 2015. Yellow star on inset map marks the location of the local map. Letters correspond to mountain ID (V=Vallunaraju, I=Ishinca, U=Urus Este, T=Tocllaraju, Y=Yannapacha, P=Pisco, A=Alpamayo). Full site descriptions provided in Table 1. Red circles indicate Near and Far grouping based on distance from Huaraz.

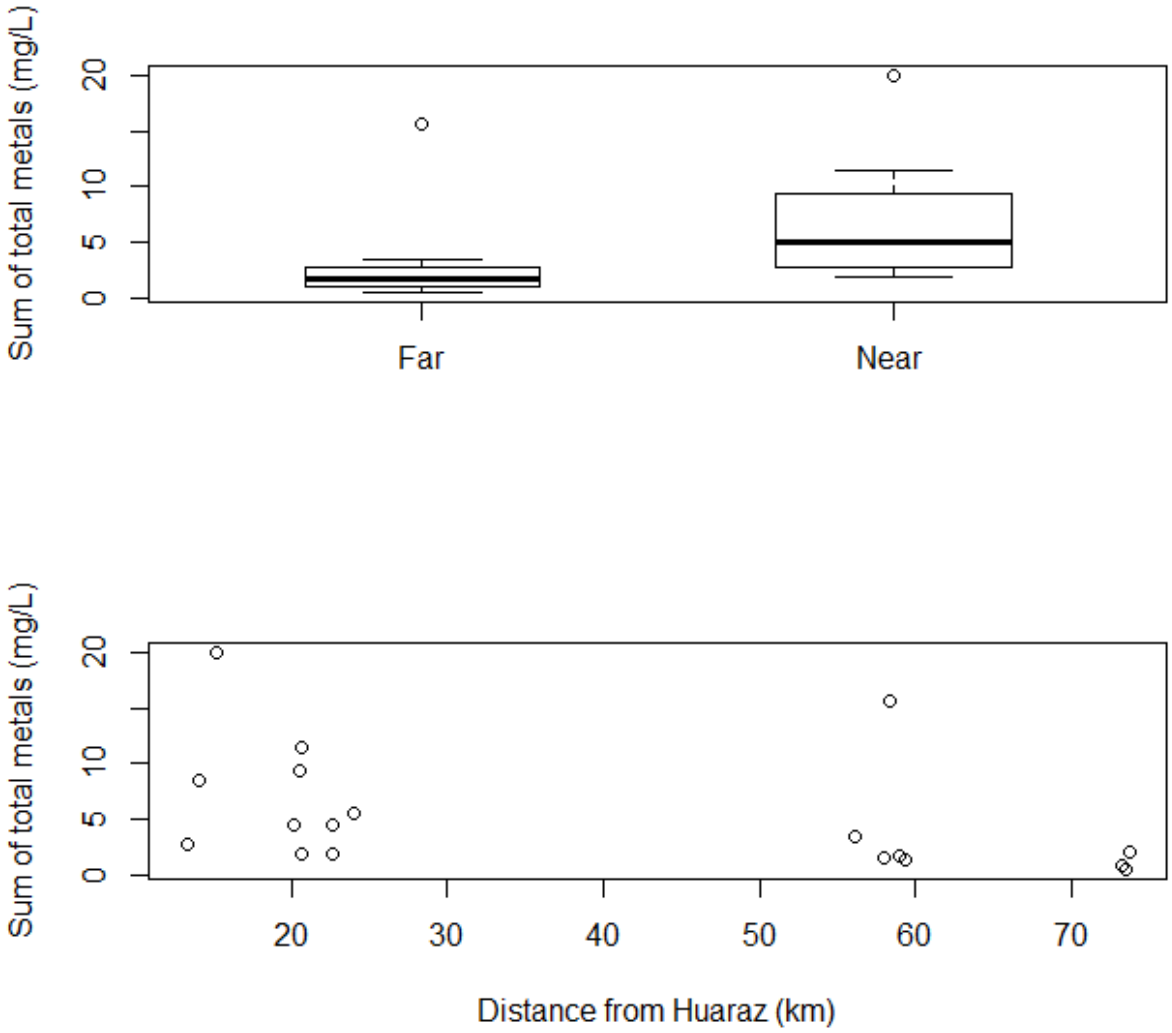

Figure 2. Top: Boxplot showing a significant difference ($p<0.05$, Kruskal-Wallis) in the summed total metals for Near samples (n=12) and Far samples (n=8). Open circles represent outliers (P2 in Far samples and V1 in Near samples [Table 1]). Bottom: Scatterplot showing no significant linear relationship ($p>0.05$) between distance from Huaraz and the total metal sum.

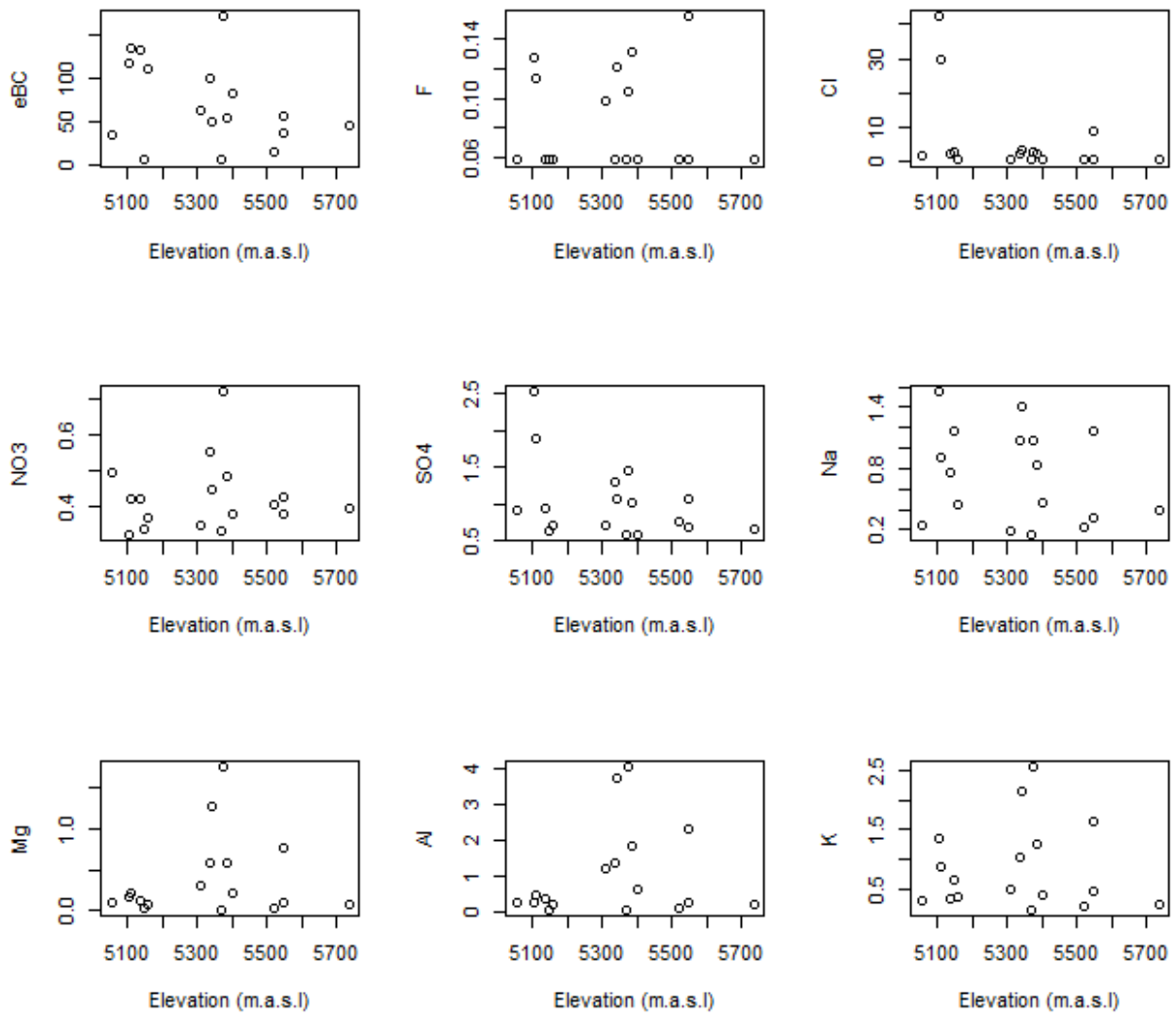

Figure 3. Scatterplots showing no significant linear relationship between elevation and any of the measured variables ($p>0.05$) for Combined samples.

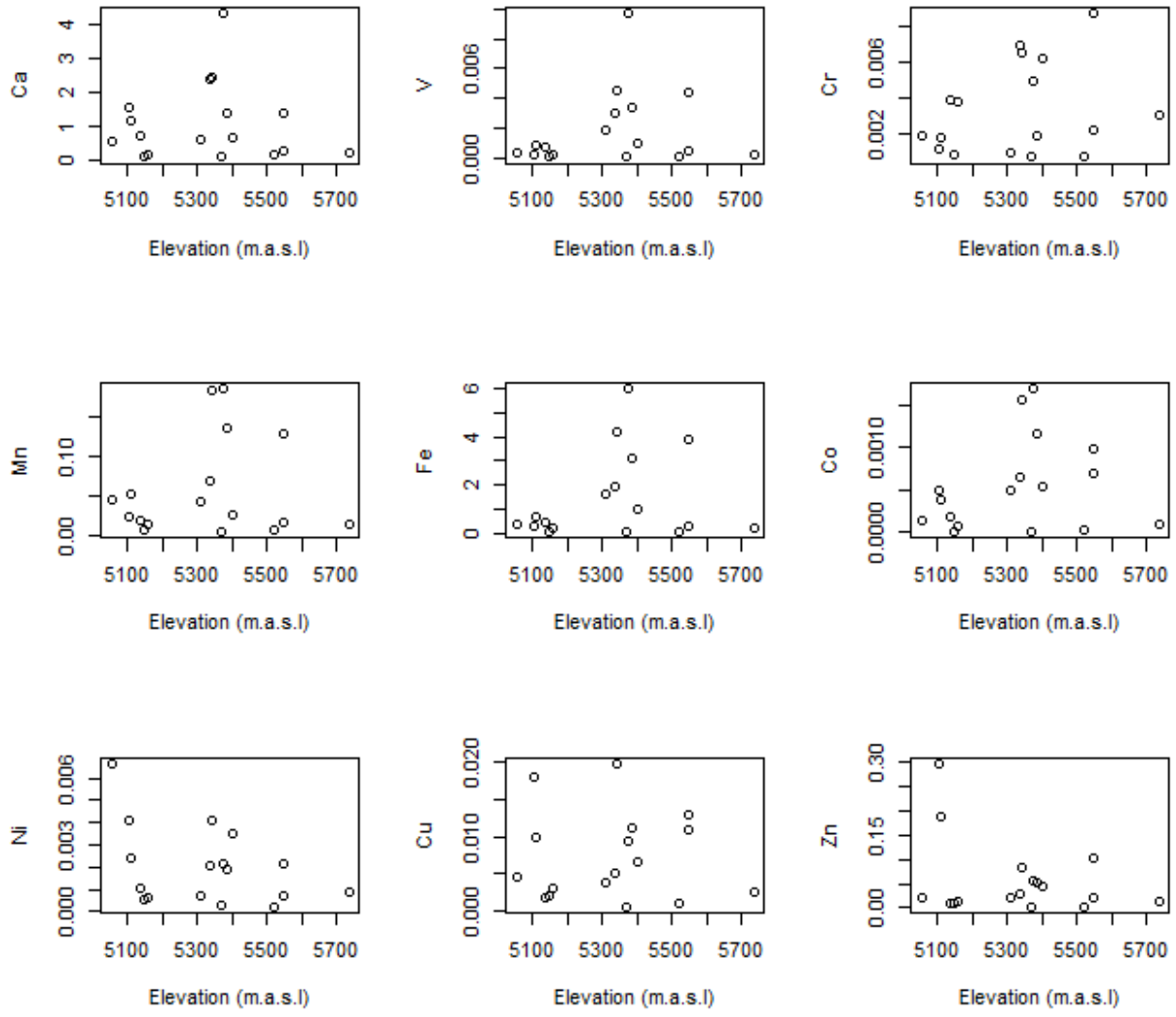

Figure 3 (continued).

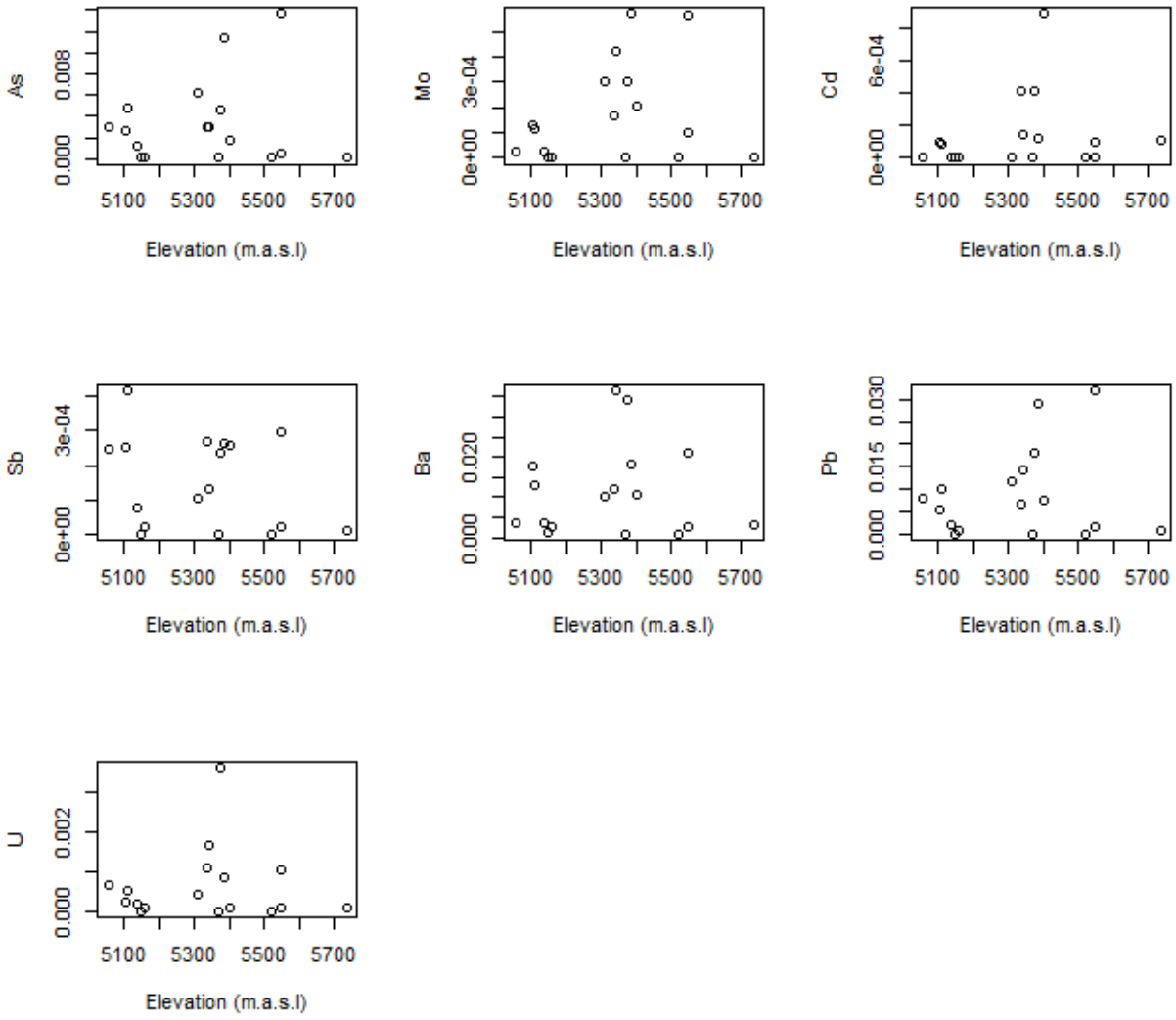

Figure 2 (continued).

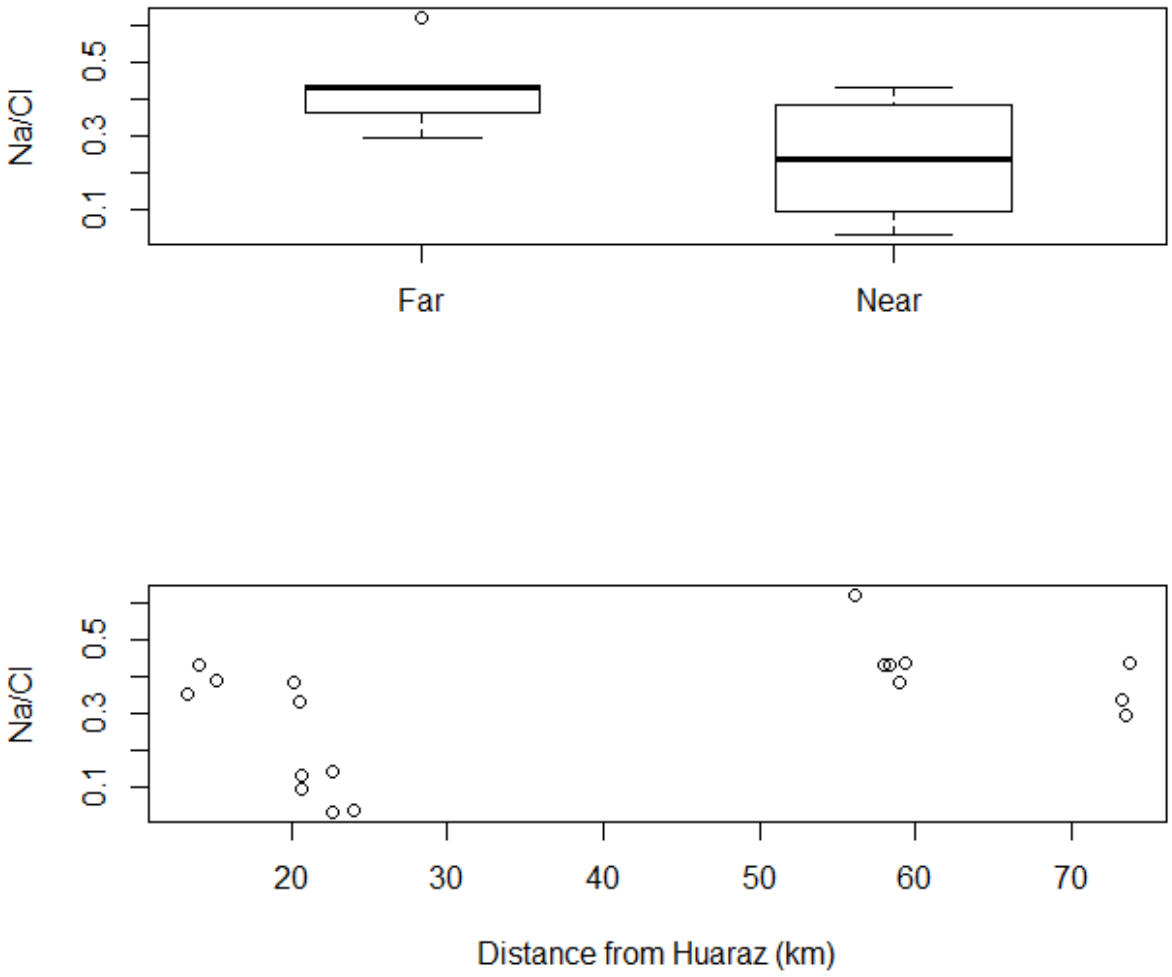

Figure 4. Boxplot showing a significant difference ($p<0.05$, Kruskal-Wallis) between the Na/Cl ratio for Near samples (n=12) and Far samples (n=8) (top), and scatterplot showing no significant ($p>0.05$) linear relationship between the distance and the Na/Cl ratio for Combined samples.

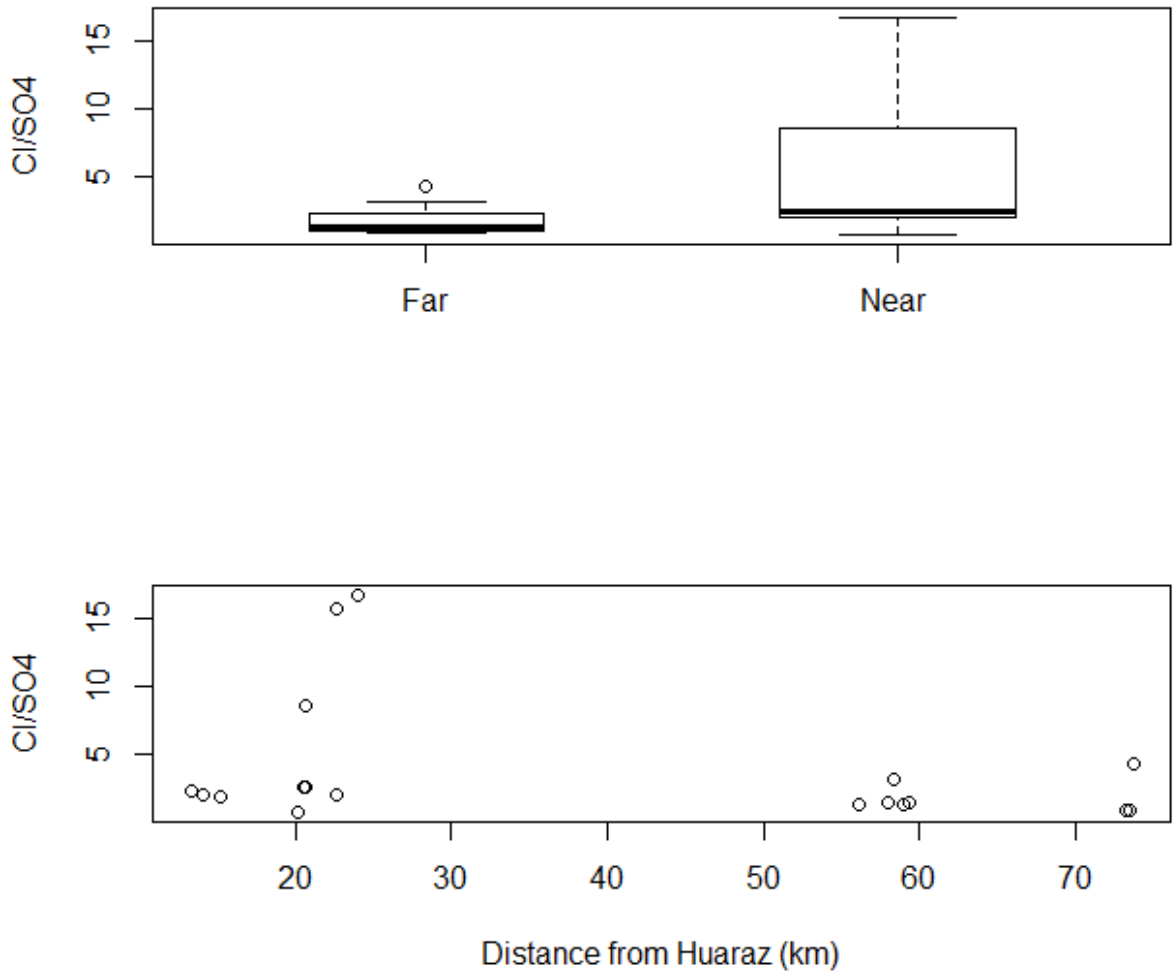

Figure 5. Boxplot showing no significant difference ($p>0.05$, Kruskal-Wallis) in the ratio of Cl/SO_4 for Near samples (n=12) and Far samples (n=8) (top), and scatterplot showing no significant linear relationship ($p>0.05$) between Cl/SO_4 ratio and distance from Huaraz with Combined samples (bottom).

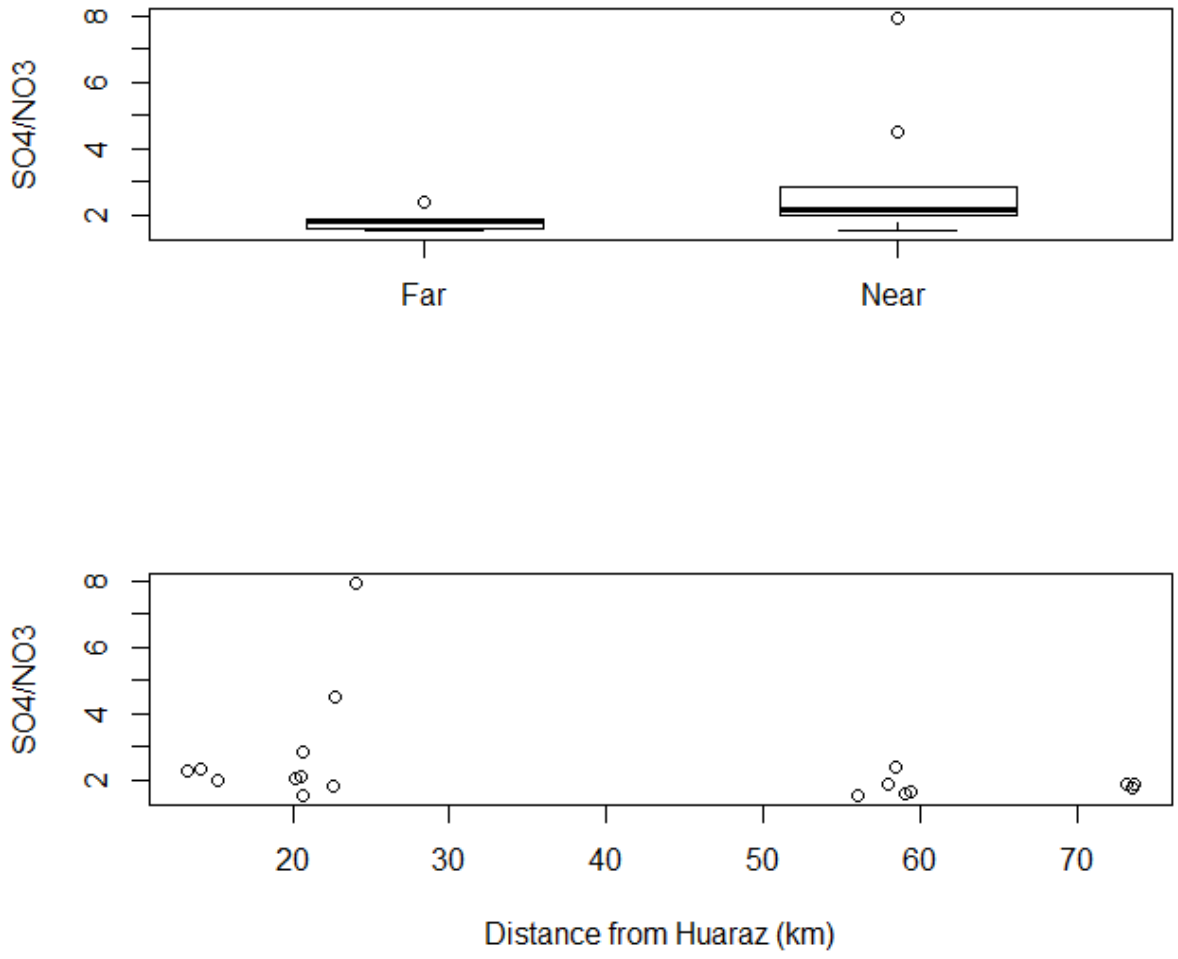

Figure 6. Boxplot showing significant difference in ratios of SO_4/NO_3 ($p<0.05$, Kruskal-Wallis) for Near samples (n=12) and Far samples (n=8) (top), and scatterplot showing no significant linear relationship with SO_4/NO_3 and distance from Huaraz with Combined samples (bottom).

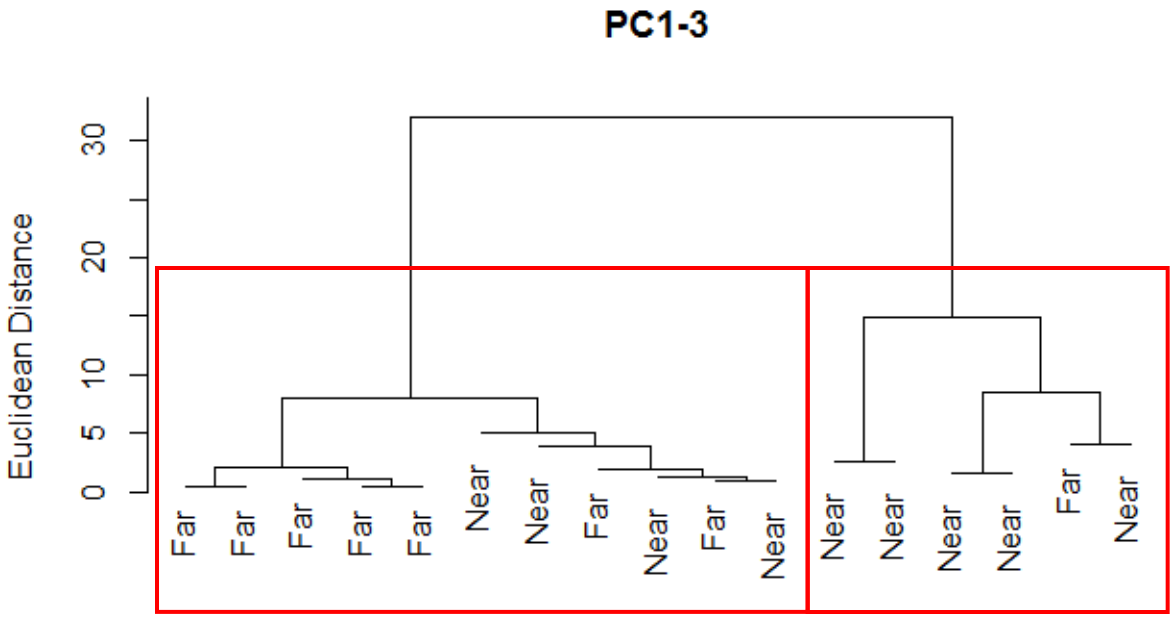

Figure 7. Hierarchical clustering on the first three principal components (PC1-3), as described in Table 7, labeled based on Near and Far samples. Two distinct groups are shown with manually created red boxes, which correspond to Group 1 (G1; left box) and Group 2 (G2; right box) as determined from "cutree" in R.

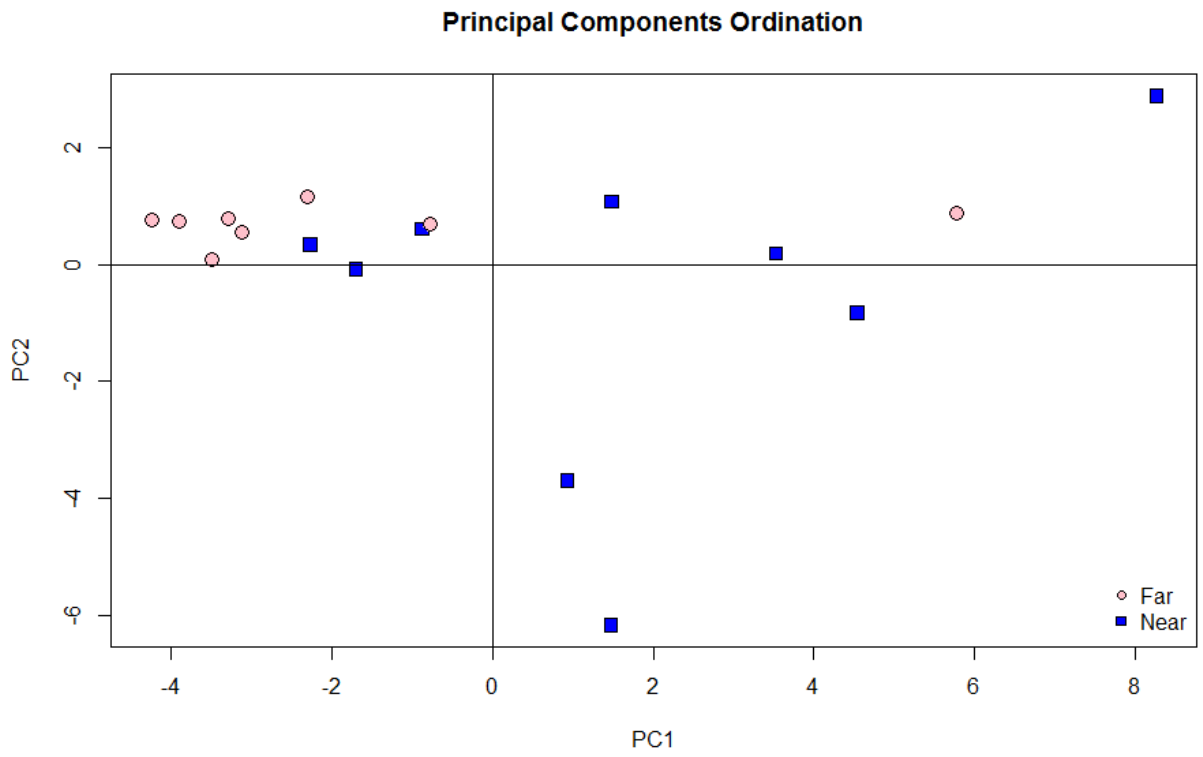

Figure 8. Principal components ordination of Near samples (blue squares) and Far samples (pink circles) graphed on principal component 1 (PC1) and principal component 2 (PC2).

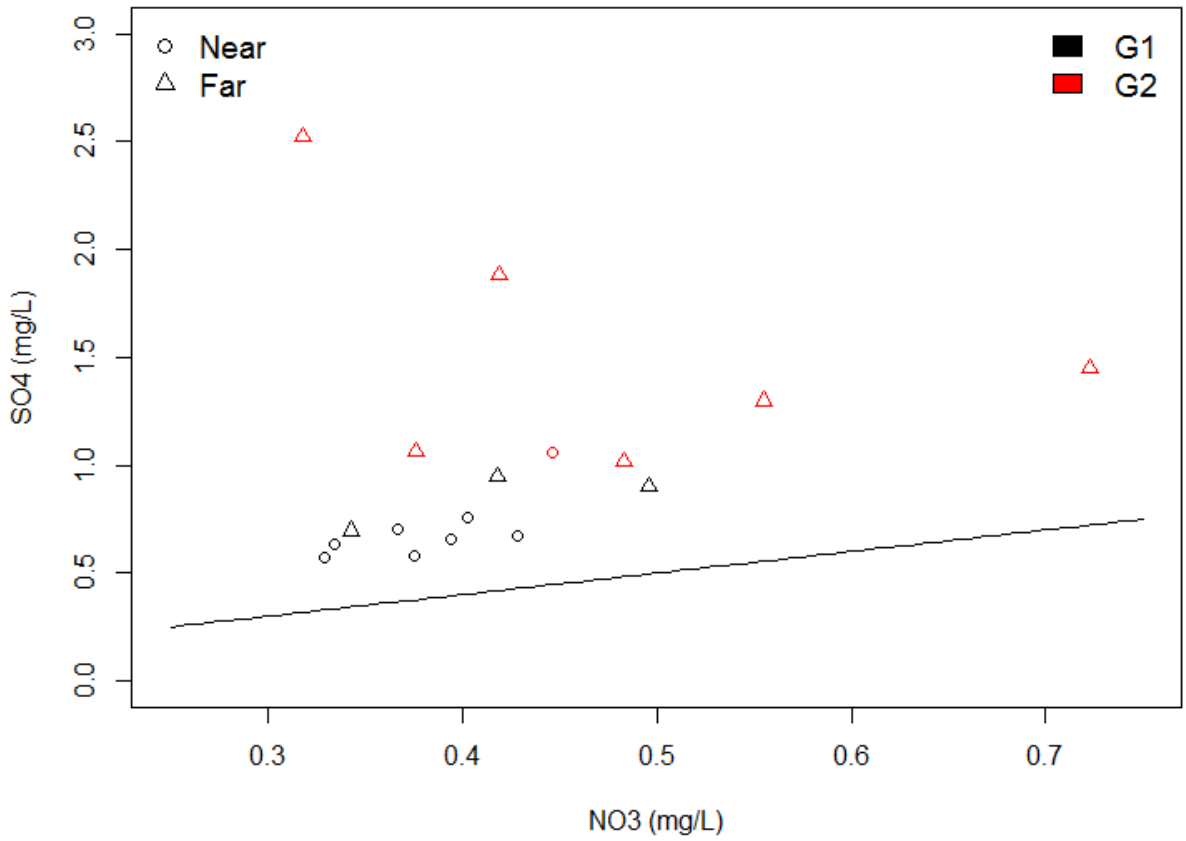

Figure 9. Scatterplot of SO_4/NO_3 ratios for Combined samples, classified as Near (open circles; n=12) or Far (open triangles; n=8) and Group 1 (black) or Group 2 (red). Solid line indicates a SO_4/NO_3 ratio of one.

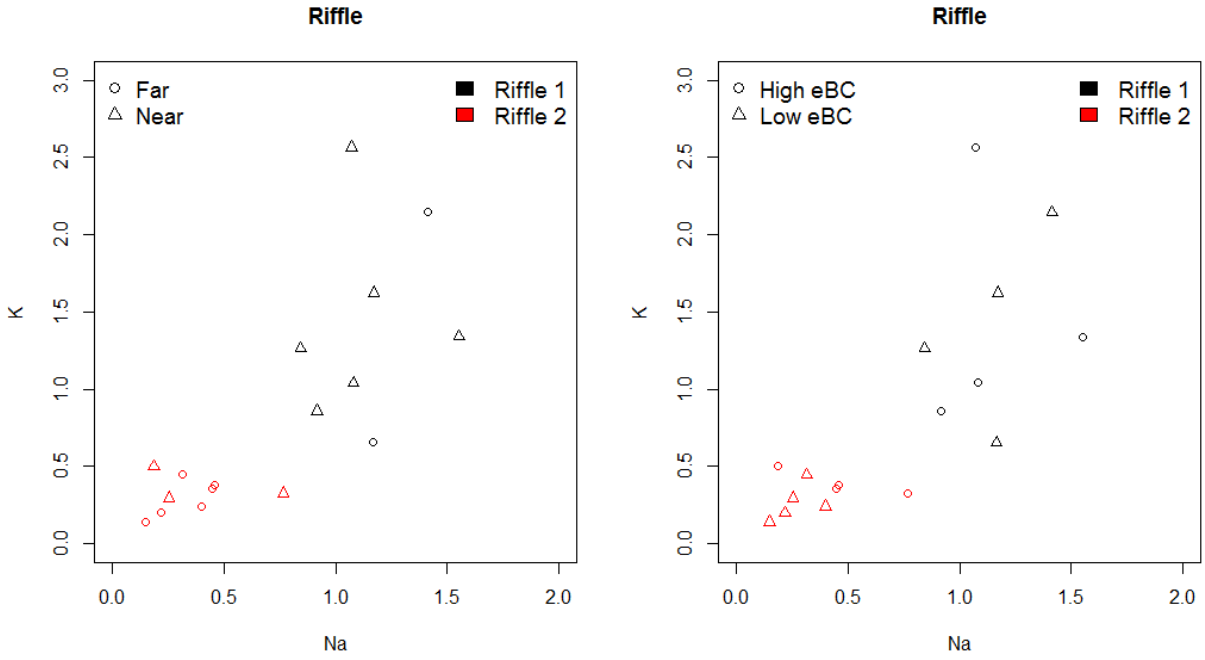

Figure 10. RIFFLE clustering plotted on Na and K for classifications on Near vs. Far samples (left), or High vs. Low eBC (right). There was not a significant association between groups (Riffle 1 and Riffle 2) and distance or eBC categories ($p>0.05$, Pearson's Chi-squared test with Yates' continuity correction).

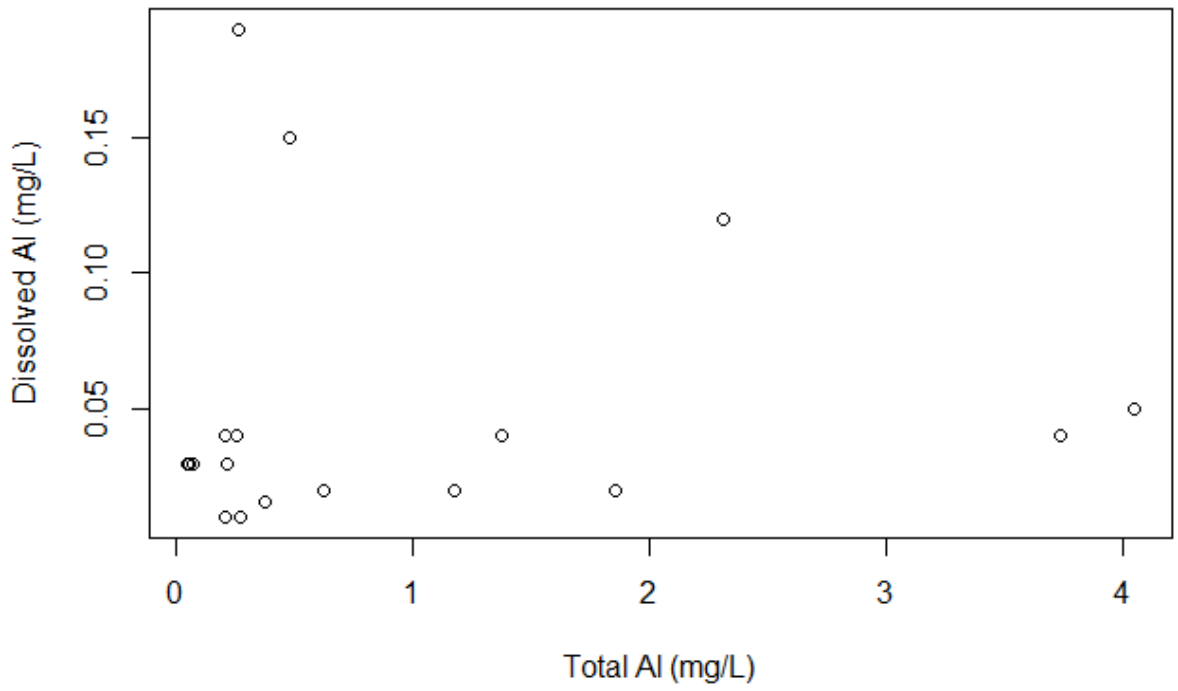

Figure 11. Scatterplot of total vs. dissolved Al. There was no significant linear relationship ($p>0.05$).

Tables

Table 1. Descriptions of sampling locations. An estimated aspect of "NA" refers to a summit sample. Site classifications are categorical descriptions of the mountains based on distance from Huaraz.

Mountain	Site classification	Sample ID	Latitude	Longitude	Elevation (m.a.s.l.)	Estimated aspect
Ishinca	Near	I1	-9.396309257	-77.40828747	5385	W
		I2	-9.398307418	-77.4132177	5308	NW
		I3	-9.392247386	-77.40612687	5548	NA
Tocllaraju	Near	T1	-9.354137974	-77.41291386	5105	SE
Urus Este	Near	U1	-9.355131984	-77.43378849	5052	SE
		U2	-9.354781033	-77.43572764	5108	NA
Vallunaraju	Near	V1	-9.421181884	-77.45640253	5374	NA
		V2	-9.431177387	-77.45973467	5337	W
		V3	-9.436304765	-77.46245636	5138	W
Alpamayo	Far	A1	-8.883873224	-77.65655969	5145	SE
		A2	-8.882718617	-77.65639583	5370	NW
		A3	-8.885947997	-77.65532931	5522	SW
Pisco	Far	P1	-9.018692449	-77.64362139	5160	S
		P2	-9.013685938	-77.64283223	5342	N
		P3	-9.012063453	-77.63631103	5547	NW
		P4	-9.009572603	-77.63234069	5735	NA
Yannapacha	Far	Y1	-9.027028587	-77.57666163	5400	W

Table 2. Median concentrations of analytes (ng/g for eBC and mg/L for all other chemical analytes). Bolded variables and values indicates a statistically significant ($p<0.05$, Kruskal-Wallis) between Near samples (n=12) and Far samples (n=8).

	Near	Far
eBC	**80.2**	**41**
Cl	2.34	0.872
SO_4	**1.04**	**0.664**
Ca	**0.944**	**0.225**
Na	0.804	0.422
K	0.679	0.365
Fe	0.667	0.227
Al	0.485	0.214
NO_3	0.418	0.384
Mg	0.226	0.073
F	0.102	0.058
Mn	**0.0439**	**0.0135**
Zn	0.024	0.0136
Ba	0.0111	0.0026
Pb	**0.00733**	**0.000804**
Cu	0.00487	0.00284
As	**0.00304**	**0.000211**
Ni	0.00201	0.00065
Cr	0.00178	0.00345

Table 3. Correlation coefficients of eBC and common soil markers for (a) Combined samples, (b) Near samples (n=12), and (c) Far samples (n=8). Bold values indicate a significant correlation ($p<0.05$; Kendall's τ).

a.

	eBC	Mg	Al	Ca	Mn	Fe
Mg	**0.40**					
Al	**0.38**	**0.93**				
Ca	**0.50**	**0.81**	**0.77**			
Mn	0.32	**0.90**	**0.88**	**0.77**		
Fe	0.35	**0.93**	**0.97**	**0.77**	**0.88**	
Co	0.27	**0.85**	**0.80**	**0.72**	**0.78**	**0.83**

b.

	eBC	Mg	Al	Ca	Mn	Fe
Mg	0.06					
Al	0.06	**0.89**				
Ca	0.39	**0.56**	0.44			
Mn	-0.11	**0.72**	**0.72**	0.39		
Fe	0.06	**0.89**	**1.00**	0.44	**0.72**	
Co	-0.06	**0.89**	**0.78**	**0.56**	**0.72**	**0.78**

c.

	eBC	Mg	Al	Ca	Mn	Fe
Mg	0.57					
Al	**0.64**	**0.93**				
Ca	0.50	**0.93**	**0.86**			
Mn	0.57	**1.00**	**0.93**	**0.93**		
Fe	0.57	**1.00**	**0.93**	**0.93**	**1.00**	
Co	0.47	**0.91**	**0.84**	**0.84**	**0.91**	**0.91**

Table 4. Correlation coefficients of eBC and common fuel combustion for (a) Combined samples, (b) Near samples (n=12), and (c) Far samples (n=8). Bold values indicate a significant correlation ($p<0.05$).

a.

	eBC	NO_3	SO_4	K	V	Ni	Cu	Zn	As	Sb
NO_3	0.15									
SO_4	**0.50**	**0.38**								
K	0.32	0.21	**0.47**							
V	**0.38**	**0.41**	**0.44**	**0.68**						
Ni	0.31	0.31	**0.46**	**0.40**	**0.46**					
Cu	0.25	0.22	**0.46**	**0.66**	**0.54**	**0.53**				
Zn	**0.41**	0.21	**0.59**	**0.62**	**0.56**	**0.63**	**0.78**			
As	0.35	0.32	**0.47**	**0.50**	**0.71**	**0.46**	**0.52**	**0.59**		
Sb	**0.42**	0.31	**0.54**	**0.44**	**0.57**	**0.56**	**0.54**	**0.68**	**0.69**	
Pb	0.30	**0.36**	**0.42**	**0.54**	**0.78**	**0.49**	**0.55**	**0.63**	**0.86**	**0.65**

b.

	eBC	NO_3	SO_4	K	V	Ni	Cu	Zn	As	Sb
NO_3	0.06									
SO_4	0.44	0.06								
K	0.22	0.06	0.44							
V	0.06	0.33	0.06	**0.61**						
Ni	0.00	0.17	**0.56**	0.11	-0.17					
Cu	0.00	-0.17	**0.56**	**0.56**	0.17	0.33				
Zn	0.22	-0.17	**0.67**	**0.56**	0.17	0.44	**0.78**			
As	-0.33	-0.06	-0.11	0.22	0.50	-0.11	0.33	0.22		
Sb	-0.06	0.00	0.39	0.17	0.11	0.28	0.50	0.50	0.28	
Pb	-0.22	0.06	-0.11	0.33	**0.61**	-0.11	0.33	0.22	**0.89**	0.28

c.

	eBC	NO_3	SO_4	K	V	Ni	Cu	Zn	As	Sb
NO_3	0.21									
SO_4	0.29	**0.64**								
K	0.21	0.29	0.21							
V	**0.64**	0.57	0.36	0.57						
Ni	0.50	0.43	0.07	0.43	**0.71**					
Cu	0.50	0.57	0.36	**0.71**	**0.86**	**0.71**				
Zn	0.50	0.57	0.21	0.57	**0.86**	**0.86**	**0.86**			
As	**0.64**	0.57	0.36	0.57	**1.00**	**0.71**	**0.86**	**0.86**		
Sb	**0.64**	0.42	0.19	0.49	**0.87**	**0.72**	**0.79**	**0.79**	**0.87**	
Pb	0.55	**0.62**	0.26	0.47	**0.91**	**0.76**	**0.76**	**0.91**	**0.91**	**0.81**

Table 5. Correlation coefficients of eBC and common sea salt/marine markers for (a) Combined samples, (b) Near samples (n=12), and (c) Far samples (n=8). Bold values indicate a significant correlation ($p<0.05$).

a.

	eBC	Cl	SO_4	Na
Cl	0.34			
SO_4	**0.50**	**0.66**		
Na	0.35	**0.75**	**0.47**	
Mg	**0.40**	0.35	**0.49**	**0.43**

b.

	eBC	Cl	SO_4	Na
Cl	0.28			
SO_4	0.44	**0.83**		
Na	0.22	**0.72**	**0.67**	
Mg	0.06	0.22	0.17	0.28

c.

	eBC	Cl	SO_4	Na
Cl	0.36			
SO_4	0.29	0.36		
Na	0.43	**0.79**	0.14	
Mg	0.57	0.21	0.29	0.43

Table 6. Median concentrations of analytes (in mg/L) for High and Low eBC categories. High eBC indicates a value greater than 50 ng/g and Low eBC is less than 50 ng/g. Bolded values indicate a significant difference between High eBC and Low eBC ($p<0.05$, Kruskal-Wallis).

	High eBC	**Low eBC**
Ca	**1.14**	**0.303**
Fe	**0.984**	**0.146**
K	0.858	0.24
Na	0.844	0.253
Al	**0.628**	**0.118**
Mg	**0.226**	**0.053**
Mn	**0.0431**	**0.0085**
Zn	**0.0431**	**0.0083**
Ba	**0.0123**	**0.00176**
Pb	**0.0077**	**0.000702**
Cu	0.0067	0.00215
As	**0.003**	**0.000378**
Cr	0.0022	0.00145
Ni	0.0021	0.000515

Table 7. Variable loadings for PCA in descending order based on principal components (PCs).

	PC1		**PC2**		**PC3**		**PC4**		**PC5**
Ba	0.260	NO_3	0.225	eBC	0.360	Na	0.194	Cu	0.451
K	0.258	Cr	0.203	Cr	0.311	K	0.190	Cr	0.442
Mn	0.255	V	0.178	Cd	0.260	U	0.149	Na	0.219
Co	0.253	U	0.159	NO_3	0.256	SO_4	0.135	Co	0.186
Fe	0.251	Al	0.158	SO_4	0.209	Mg	0.126	Ba	0.149
Mg	0.250	Fe	0.157	Ca	0.208	V	0.110	K	0.100
Al	0.248	Mg	0.153	U	0.130	Ca	0.107	Ni	0.086
Ca	0.246	Mn	0.108	Ni	0.129	Al	0.095	Al	0.081
V	0.242	Co	0.101	Cl	0.115	Cl	0.092	Mo	0.078
U	0.234	Cd	0.096	Na	0.088	F	0.071	Zn	0.066
Mo	0.216	Ca	0.058	Zn	0.085	Ba	0.057	Mn	0.039
Pb	0.215	Mo	0.022	Mg	0.053	Fe	0.055	Cd	0.037
F	0.207	K	-0.004	Sb	0.045	Zn	0.035	Mg	0.018
Cu	0.199	Ba	-0.005	K	0.030	Mn	0.033	F	0.006
Na	0.181	Pb	-0.008	V	0.025	eBC	0.028	Cl	-0.032
Sb	0.174	As	-0.069	Ba	0.018	NO_3	-0.004	Fe	-0.036
As	0.174	eBC	-0.100	Co	-0.018	Co	-0.008	Ca	-0.091
NO_3	0.167	Ni	-0.158	Cu	-0.024	Cu	-0.038	SO_4	-0.130
SO_4	0.136	Na	-0.204	Al	-0.036	Mo	-0.170	V	-0.138
eBC	0.132	Cu	-0.205	Fe	-0.077	Pb	-0.186	Pb	-0.146
Zn	0.114	Sb	-0.211	Mn	-0.091	As	-0.193	U	-0.169
Ni	0.110	F	-0.212	F	-0.284	Cr	-0.258	As	-0.242
Cd	0.096	SO_4	-0.367	Mo	-0.331	Sb	-0.422	Sb	-0.298
Cr	0.073	Zn	-0.429	Pb	-0.337	Ni	-0.428	NO_3	-0.303
Cl	0.060	Cl	-0.460	As	-0.406	Cd	-0.533	eBC	-0.351

Table 8. Median values for variables in cluster Groups 1 (G1) and 2 (G2) and analyte concentration for P2 (the lone Far sample in G2), as shown in Figure 8. Concentrations are reported in ng/g for eBC and mg/L for all other analytes.

	G1	**P2**	**G2**
eBC	44.6	48.8	86.0
Cl	0.921	3.28	6.17
Fe	0.282	4.17	3.51
Al	0.256	3.73	2.08
Ca	0.303	2.46	1.49
K	0.354	2.15	1.48
SO_4	0.698	1.06	1.26
Na	0.399	1.41	1.12
Mg	0.099	1.27	0.68
NO_3	0.394	0.446	0.43
Mn	0.016	0.184	0.13
F	0.058	0.121	0.12
Zn	0.014	0.0838	0.09
Ba	0.003	0.0365	0.02
Pb	0.002	0.0144	0.02
Cu	0.003	0.0199	0.01
Cr	0.0030	0.0065	0.0020
Ni	0.0010	0.0041	0.0023
As	0.0004	0.0030	0.0047
V	0.0004	0.0045	0.0039
Co	0.0001	0.0016	0.0011
U	0.0001	0.0017	0.0009
Mo	0.00003	0.0004	0.0004
Sb	0.00003	0.0001	0.0003
Cd	0.0000	0.0001	0.0001

Table 9. Correlation coefficients (τ) and associated p-values for total and dissolved metals. Bolded variables are those that had a significant ($p<0.05$, Kruskal-Wallis) correlation between total and dissolved.

Metal	τ	p-value
Na	**0.817**	**1.28E-7**
Mg	**0.669**	**2.70E-05**
Al	0.193	0.229
K	**0.612**	**8.39E-05**
Ca	**0.747**	**1.37E-06**
V	0.206	0.215
Cr	-0.0265	0.876
Mn	**0.444**	**0.0046**
Fe	**0.357**	**0.0278**
Co	0.252	0.12
Ni	**0.738**	**1.81E-06**
Cu	**0.464**	**0.00275**
Zn	**0.572**	**0.000216**
As	**0.651**	**2.57E-05**
Se	0.0792	0.652
Mo	**0.47**	**0.00879**
Cd	0.188	0.284
Sb	**0.661**	**2.40E-05**
Ba	**0.511**	**0.000952**
Pb	**0.371**	**0.0296**
U	**0.43**	**0.0122**

References

Agency for Toxic Substances and Disease Registry (ATSDR). 2012. Toxicological profile for Vanadium. Atlanta, GA: U.S. Department of Health and Human Services, Public Health Service.

Almeida S.M., C.A. Pio, M.C. Freitas, M.A. Trancoso. 2006. Approaching PM2.5 and PM2.5-10 source apportionment by mass balance analysis, principal component analysis and particle size distribution. Science of the Total Environment 368:663-674.

Al-Khashman O.A. 2009. Chemical characteristics of rainwater collected at a western site of Jordan. Atmospheric Research 91:53–61.

Baraer M., B.G. Mark, J.M. McKenzie, T. Condom, J. Bury, K.-I. Huh, C. Portocarrero, J. Gómez, S. Rathay. 2012. Glacier recession and water resources in Peru's Cordillera Blanca. Journal of Glaciology 58:134-150.

Barnet T.P., J.C. Adam, D.P. Lettenmaier. 2005. Potential impacts of a warming climate on water availability in snow-dominated regions. Nature 438:303-309.

Bodenlos A.J. and Ericksen G.E. 1955. Lead-zinc deposits of Cordillera Blanca and northern Cordillera Huayhuash, Peru. United States Geological Survey Bulletin 1017, 102 p.

Bond T.C., S.J. Doherty, D.W. Fahey, P.M. Forster, T. Berntsen, B.J. DeAngelo, M.G. Flanner, S. Ghan, B. Kärcher, D. Koch, S. Kinne, Y. Kondo, P.K. Quinn, M.C. Sarofim, M.G. Schultz, M. Schulz, C. Venkataraman, H. Zhang, S. Zhang, N. Bellouin, S.K. Guttikunda, P.K. Hopke, M.Z. Jacobson, J.W. Kaiser, Z. Klimont, U. Lohmann, J.P. Schwarz, D. Shindell, T. Storelvmo, S.G. Warren, C.S. Zender. 2013. Bounding the role of black carbon in the climate system: A scientific assessment. Journal of Geophysical Research: Atmospheres 118:5380–5552.

Burgess G.L. 2015. Effects of heavy metals on benthic macroinvertebrates in the Cordillera Blanca, Peru (Master's Thesis). Retrieved from Western Washington University's Master's Thesis Collection: http://cedar.wwu.edu/wwuet/.

Colbeck S.C. 1981. A simulation of the enrichment of atmospheric pollutants in snow cover runoff. Water Resources Research 17.5:1383-1388.

Davies T.D., P. Brimblecombe, M. Tranter, S. Tsiouris, C.E. Vincent, P. Abrahams, I.L. Blackwood. 1987. The removal of soluble ions from melting snowpacks. Seasonal Snowcovers: Physics, Chemistry, Hydrology, NATO ASI Series C: Math and Phys. Sci., ed. H.G. Jones and W.J. Orville-Thomas. 211:337-392.

de Caritat P., G. Hall, S. Gìslason, W. Belsey, M. Braun, N.I. Goloubeva , H.K. Olsen, J.O. Scheie, J.E. Vaive. 2005. Chemical composition of arctic snow: concentration levels and regional distribution of major elements. Science of the Total Environment 336:183-199.

Doherty S.J., T.C. Grenfell, S. Forsström, D.L. Hegg, R.E. Brandt, S.G. Warren. 2013. Observed vertical redistribution of black carbon and other insoluble light-absorbing particles in melting snow. Journal of Geophysical Research: Atmospheres 118:5553–5569.

Dore A.J., T.W. Choularton, D. Fowler, A. Crossley. 1992. Orographic enhancement of snowfall. Environmental Pollution 75:175–179.Esri. 2015. ArcGIS desktop 10.3.1.

Evans M., N. Kholod, V. Malyshev, S. Tretyakova, E. Gusev, S. Yu, A. Barinov. 2015. Black carbon emissions from Russian diesel sources: case study of Murmansk. Atmospheric Chemistry and Physics 15:8349–8359.

Fortner S.K., B.G. Mark, J.M. McKenzie, J. Bury, A. Trierweiler, M. Baraer, P. J. Burns, L. Munk. 2011. Elevated stream trace and minor element concentrations in the foreland of receding tropical glaciers. Applied Geochemistry 26:1792–1801.

Gabrielli P., G. Cozzi, S. Torcini, P. Cescon, C. Barbante. 2006. Source and origin of atmospheric trace elements entrapped in winter snow of the Italian Eastern Alps. Atmospheric Chemistry and Physics Discussions 6:8781–8815.

Gandy C.J., J.W.N. Smith, A.P. Jarvis. 2007. Attenuation of mining-derived pollutants in the hyporheic zone: a review. Science of the Total Environment 373.2:435-446.

Grenfell T.C., D.K. Perovich, J.A. Ogren. 1981. Spectral albedos of an alpine snowpack. Cold Regions Science and Technology 4:121–127.

Grenfell T. C., S.G. Warren, V.F. Radionov, V.N. Makarov, S.A. Zimov. 2009. Expeditions to the Russian Arctic to survey black carbon in snow. Eos, Transactions American Geophysical Union 90:386–387.

Grigholm B., P.A. Mayewski, A.V. Kurbatov, G. Casassa, A.C. Staeding, M. Handley, S.B. Sneed, D.S. Introne. 2009. Chemical composition of fresh snow from Glaciar Marinelli, Tierra del Fuego, Chile. Journal of Glaciology 55:769–776.

Hadley O.L., C.E. Corrigan, T.W. Kirchstetter, S.S. Cliff, V. Ramanathan. 2010. Measured black carbon deposition on the Sierra Nevada snowpack and implication for snow pack retreat. Atmospheric Chemistry and Physics 10:7505-7513.

Hansen J. and L. Nazarenko. 2004. Soot climate forcing via snow and ice albedos. Proceedings of the National Academy of Sciences 101:423-428.

Hegg D.A., S.G. Warren, T.C. Grenfell, S.J. Doherty, T.V. Larson, A.D. Clarke. 2009. Source attribution of black carbon in arctic snow. Environmental Science and Technology 43:4016-4021.

Hegg, D.A., S.G. Warren, T.C. Grenfell, S.J. Doherty, A.D. Clarke. 2010. Sources of light-absorbing aerosol in Arctic snow and their seasonal variation. Atmospheric Chemistry and Physics 10:10923–10938.

Huang J., Q. Fu, W. Zhang, X. Wang, R. Zhang, H. Ye, S.G. Warren. 2011. Dust and black carbon in seasonal snow across northern China. Bulletin of the American Meteorological Society 92:175–181.

Johannessen M., T. Dale, E.T. Gjessing, A. Henriksen, R.F. Wright. 1975. Acid precipitation in Norway: the regional distribution of contaminants in snow and the chemical concentration

processes during snowmelt. Isotopes and Impurities in Snow and Ice; XVI Assembly of the International Union of Geodesy and Geophysics 118:116–120.

Johannessen M. and A. Henriksen. 1978. Chemistry of snow meltwater: changes in concentration during melting. Water Resources Research 14:615-619.

Juen I., G. Kaser, C. Georges. 2007. Modelling observed and future runoff from a glacierized tropical catchment (Cordillera Blanca, Perú). Global and Planetary Change 59:37-48.

Kang S., Q. Zhang, S. Kaspari, D. Qin, Z. Cong, J. Ren, P.A. Mayewski. 2007. Spatial and seasonal variations of elemental composition in Mt. Everest (Qomolangma) snow/firn. Atmospheric Environment 41:7208-7218.

Kaser G., A. Ames, and M. Zamora. 1990. Glacier fluctuations and climate in the Cordillera Blanca, Peru. Annals of Glaciology 14:136-140.

Kaser G. and C. Georges. 1999. On the mass balance of low latitude glaciers with particular consideration of the Peruvian Cordillera Blanca. Geografiska Annaler: Series A, Physical Geography 81:643–651.

Kopp R.E. and D.L. Mauzerall. 2010. Assessing the climatic benefits of black carbon mitigation. Proceedings of the National Academy of Sciences of the United States of America 107:11703-11708.

Kroopnick P. 1977. The SO_4:Cl ratio in oceanic rainwater. Pacific Science 31:91-106.

Kuhn M. 2001. The nutrient cycle through snow and ice, a review. Aquatic Science 63:150–167.

Larose C., A. Dommergue, T.M. Vogel. 2013. The dynamic arctic snow pack: an unexplored environment for microbial diversity and activity. Biology 2:317–330.

Lipten E.J. and S.W. Smith. 2005. The Geology of the Antamina Copper-Zinc Deposit, Peru, South America. In: Porter T.M. (ed) Super Porphyry Copper & Gold Deposits: A Global Perspective, PGC Publishing, Adelaide, vol. 1, pp. 189-204.

Losno R., J.L. Colin, N. Le Bris, G. Bergametti, T. Jickells, B. Lim. 1993. Aluminium solubility in rainwater and molten snow. Journal of Atmospheric Chemistry 17:29-43.

Love D.A., A.H. Clark, J.K. Glover. 2004. The lithologic, stratigraphic, and structural setting of the giant Antamina copper-zinc skarn deposit, Ancash, Peru. Economic Geology 90:887-916.

Lovett G.M. and J.D. Kinsman. 1990. Atmospheric pollutant deposition to high-elevation ecosystems. Atmospheric Environment. Part A. General Topics 24:2767-2786.

Mark B.G. and G.O. Seltzer. 2003. Tropical glacier meltwater contribution to stream discharge: a case study in the Cordillera Blanca, Peru. Journal of Glaciology 49:271-281.

Mark B.G., J.M. McKenzie, J. Gomez. 2005. Hydrochemical evaluation of changing glacier meltwater contribution to stream discharge: Callejon de Huaylas, Peru. Hydrological Sciences Journal 50:975–987.

Mark B.G., J. Bury, J.M. McKenzie, A. French, M. Baraer. 2010. Climate change and tropical Andean glacier recession: evaluating hydrologic changes and livelihood vulnerability in the Cordillera Blanca, Peru. Annals of the Association of American Geographers 100:794-805.

Marx S.K., K.S. Lavin, K.J. Hageman, B.S. Kamber, T. O'Loingsigh, G.H. McTainsh. 2014. Trace elements and metal pollution in aerosols at an alpine site, New Zealand: sources, concentrations and implications. Atmospheric Environment 82:206-217.

Matthews G.B. and J. Hearn. 1991. Clustering without a metric. IEEE Transactions on Pattern Analysis and Machine Intelligence 13:175–184.

Matthews G.B. and R. A. Matthews. 2006. RIFFLE: an R package for Nonmetric Clustering. useR! 2006 Vienna, Austria.

McConnell J.R. and R. Edwards 2008. Coal burning leaves toxic heavy metal legacy in the Arctic. Proceedings of the National Academy of Sciences 105:12140 –12144.

Menon S., D. Koch, G. Beig, S. Sahu, J. Fasullo, D. Orlikowski. 2010. Black carbon aerosols and the third polar ice cap. Atmospheric Chemistry and Physics 10:4559-4571.

Ménégoz M., G. Krinner, Y. Balkanski, A. Cozic, O. Boucher, P. Ciais. 2013. Boreal and temperate snow cover variations induced by black carbon emissions in the middle of the 21st century. The Cryosphere 7:537-554.

Ménégoz M., G. Krinner, Y. Balkanski, O. Boucher, A. Cozic, S. Lim, P. Ginot, P. Laj, H. Gallée, P. Wagnon, A. Marinoni, H.W. Jacobi. 2014. Snow cover sensitivity to black carbon deposition in the Himalayas: from atmospheric and ice core measurements to regional climate simulations. Atmospheric Chemistry and Physics 14:4237-4249.

Molina L.T., L. Gallardo, M. Andrade, D. Baumgardner, M. Borbor-Córdova, R. Bórquez, G. Casassa, F. Cereceda-Balic, L. Dawidowski, R. Garreaud, N. Huneeus, F. Lambert, J.L. McCarty, J. McPhee, M. Mena-Carrasco, G.B. Raga, C. Schmitt, and J.P. Schwarz. 2015. Pollution and its impacts on the South American Cryosphere. Earth's Future 3:345–369.

Möller, D. 1990. The Na/Cl ratio in rainwater and the seasalt chloride cycle. Tellus B, 42(3).

Mountain Research Initiative EDW Working Group (MRI). 2015. Elevation-dependent warming in mountain regions of the world. Nature Climate Change 5:424–430.

Nagy G.J., R.M. Caffera, M. Aparicio, P. Barrenechea, M. Bidegain, J.C. Giménez, E. Lentini, G. Magrin, A.M. Murgida, C. Nobre, A. Ponce, M. Travasso, A. Villamizar, M. Wehbe. 2006. Understanding the potential impact of climate change and variability in Latin America and the Caribbean. Report prepared for the Stern Review on the Economics of Climate Change, 34 pp. http://www.sternreview.org.uk.

Pacyna J.M. and E.G. Pacyna. 2001. An assessment of global and regional emissions of trace metals to the atmosphere from anthropogenic sources worldwide. Environmental Reviews 9:269–298.

Painter T.H., M.G. Flanner, G. Kaser, B. Marzeion, R.A. VanCuren, W. Abdalati. 2013. End of the Little Ice Age in the Alps forced by industrial black carbon. Proceedings of the National Academy of Sciences 110:15216-15221.

Petford N. and M. Atherton. 1996. Na-rich partial melts from newly underplated basaltic crust: The Cordillera Blanca Batholith, Peru. Journal of Petrology 37:1491-1521.

Pouyaud B., M. Zapata, J. Yerreb, J. Gomez, G. Rosas, W. Suarez, P. Ribstein. 2005. On the future of the water resources from glacier melting in the Cordillera Blanca, Peru. Hydrological Sciences Journal-Journal Des Sciences Hydrologiques 50:999-1022.

R Core Team. 2016. R: A language and environment for statistical computing. R Foundation for Statistical Computing, Vienna, Austria. https://www.R-project.org/.

Racoviteanu A.E., Y. Arnaud, M.W. Williams, J. Ordon. 2008. Decadal changes in glacier parameters in the Cordillera Blanca, Peru, derived from remote sensing. Journal of Glaciology 54:499-510.

Schmitt C.G., J.D. All, J.P. Schwarz, W.P. Arnott, R.J. Cole, E. Lapham, A. Celestian. 2015. Measurements of light-absorbing particles on the glaciers in the Cordillera Blanca, Peru. Cryosphere 9:331–340.

Schwanck F., J.C. Simões, M. Handley, P.A. Mayewski, R.T. Bernardo, F.E. Aquino. 2016. Anomalously high arsenic concentration in a West Antarctic ice core and its relationship to copper mining in Chile, Atmospheric Environment 125:257-264.

Scotterer U., M. Grosjean, W. Stichler, P. Ginot, C. Kull, H. Bonnaveira, B. Fracou, H.W. Gaggeler, R Gallaier, G. Hoffman, B. Pouyaud, E. Ramirez, M. Schwikowski, J.D. Taupin. 2003. Glaciers and climate in the Andes between the equator and 30° S: What is recorded under extreme environmental conditions? Climatic Change 59:157-175.

Song Y., Y. Zhang, S. Xie, L. Zeng, M. Zheng, L.G. Salmon, M. Shao, S. Slanina. 2006. Source apportionment of PM2.5 in Beijing by positive matrix factorization. Atmospheric Environment 40:1526-1537.

Stern N.H. 2007. The Economics of Climate Change: The Stern Review. Cambridge University Press.

Stephan C.E., D.I. Mount, D.J. Hanson, J.H. Gentile, G.A. Chapman, W.A. Brungs. 1985. Guidelines for Deriving Numerical National Water Quality Criteria for the Protection of Aquatic Organisms and their Uses. USEPA, Office of Research and Development.

Tranter M., P.W. Abrahams, I. Blackwood, T.D. Davies, P. Brimblecombe, I.P. Thompson, C.E. Vincent. 1987. Changes in streamwater chemistry during snowmelt. Seasonal Snowcover: Physics, Chemistry, Hydrology 211:575-597.

US Environmental Protection Agency (USEPA). 1988. Ambient Water Quality Criteria for Aluminum. EPA 440/5-86-008.

US Environmental Protection Agency (USEPA). 2009. National Primary Drinking Water Regulations. EPA 816-F-09-004.

US Environmental Protection Agency (USEPA). 2011. Report to Congress on Black Carbon. http://yosemite.epa.gov/sab/sabproduct.nsf/fedrgstr_activites/05011472499C2FB28525774A0074DADE/$File/BCþRTCþExternalþPeerþReviewþDraft-opt.pdf.

US Environmental Protection Agency (USEPA). 2016. National Recommended Water Quality Criteria - Aquatic Life Criteria Table. https://www.epa.gov/wqc/national-recommended-water-quality-criteria-aquatic-life-criteria-table. Last updated on July 28, 2016. Accessed September 26, 2016.

US Environmental Protection Agency (USEPA). 2016. National Recommended Water Quality Criteria - Human Health Criteria Table. https://www.epa.gov/wqc/national-recommended-water-quality-criteria-human-health-criteria-table. Last updated on July 29, 2016. Accessed September 26, 2016.

Vuille M., G. Kaser, I. Juen. 2008. Glacier mass balance variability in the Cordillera Blanca, Peru and its relationship with climate and the large-scale circulation. Global and Planetary Change 62:14-28.

Walker T.R., S.D. Young, P.D. Crittenden, H. Zhang. 2003. Anthropogenic metal enrichment of snow and soil in north-eastern European Russia. Environmental Pollution 121:11-21.

Wang Y., G. Zhuang, A. Tang, H. Yuan, Y. Sun, S. Chen, A. Zheng. 2005. The ion chemistry and the source of PM2.5 aerosol in Beijing. Atmospheric Environment 39:3771–3784.

Wang X., W. Pu, X. Zhang, Y. Ren, J. Huang. 2015. Water-soluble ions and trace elements in surface snow and their potential source regions across northeastern China. Atmospheric Environment 114:57-65.

Warren S.G. 1984. Impurities in snow: effect on albedo and snowmelt. Annals of Glaciology 5:177-179.

Warren S.G. and W.J. Wiscombe. 1980a. A model for the spectral albedo of snow. I: pure snow. Journal of the Atmospheric Sciences 37:2712-2733.

Warren S.G. and W.J. Wiscombe. 1980b. A model for the spectral albedo of snow. II: snow containing atmospheric aerosols. Journal of the Atmospheric Sciences 37:2734-2745.

Warren S.G. and W.J. Wiscombe. 1985. Dirty snow after nuclear war. Nature 313:467–470.

Watson J.G. and J.C. Chow. 2001. Source characterization of major emission sources in the imperial and Mexicali Valleys along the US/Mexico border. Science of the Total Environment 276:33-47.

Webster J.G., D.K. Nordstrom, K.S. Smith. 1994. Transport and natural attenuation of Cu, Zn, As, and Fe in the acid mine drainage of Leviathan and Bryant Creeks. In: Alpers C.N and D.W Blowes (eds) Environmental Geochemistry of Sulfide Oxidation. American Chemical Society Symposium Series 550. ACS, Washington, DC pp. 244-260.

Wigington P.J., T.D. Davies, M. Tranter, K.N. Eshlemen. 1990. Episodic acidification of surface waters due to acidic deposition. State of Science and Technology Report 12. National Acid Precipitation Assessment Program, Washington, DC, USA.

Wright R., T. Dale, E. Gjessing, G. Hendrey, A. Henriksen, M. Johannessen, I. Muniz. 1976. Impact of acid precipitation on freshwater ecosystems in Norway. Water, Air, and Soil Pollution 6(2–4):483–499.

Ye H., R. Zhang, J. Shi, J. Huang, S.G. Warren, Q. Fu. 2012. Black carbon in seasonal snow across northern Xinjiang in northwestern China Environmental Research Letters 7:1–9.

Supplemental Information

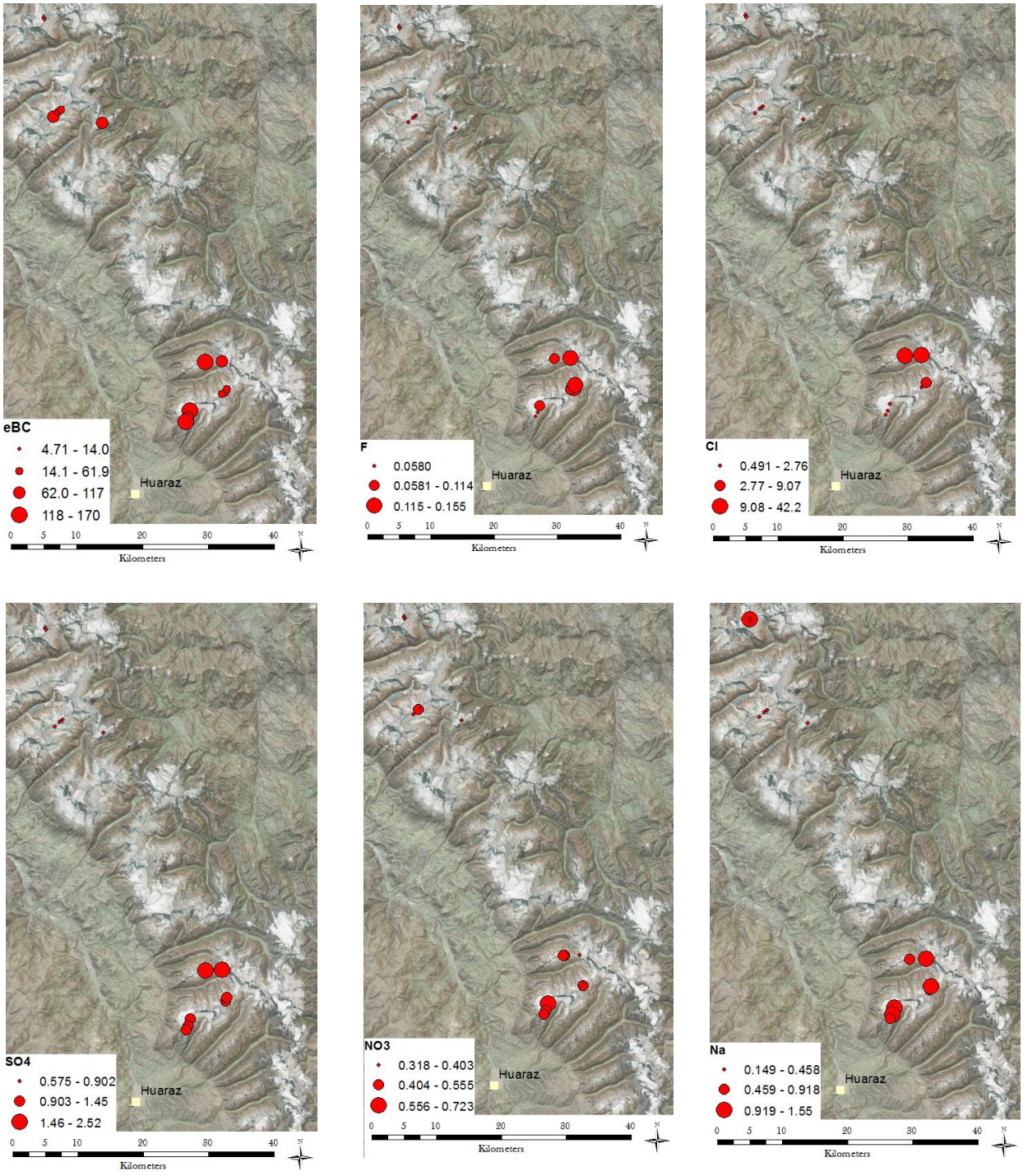

Figure S1. Spatial distribution of black carbon (eBC; ng/g) and measured analytes (mg/L). Classifications were formed based on Jenks natural breaks classification method.

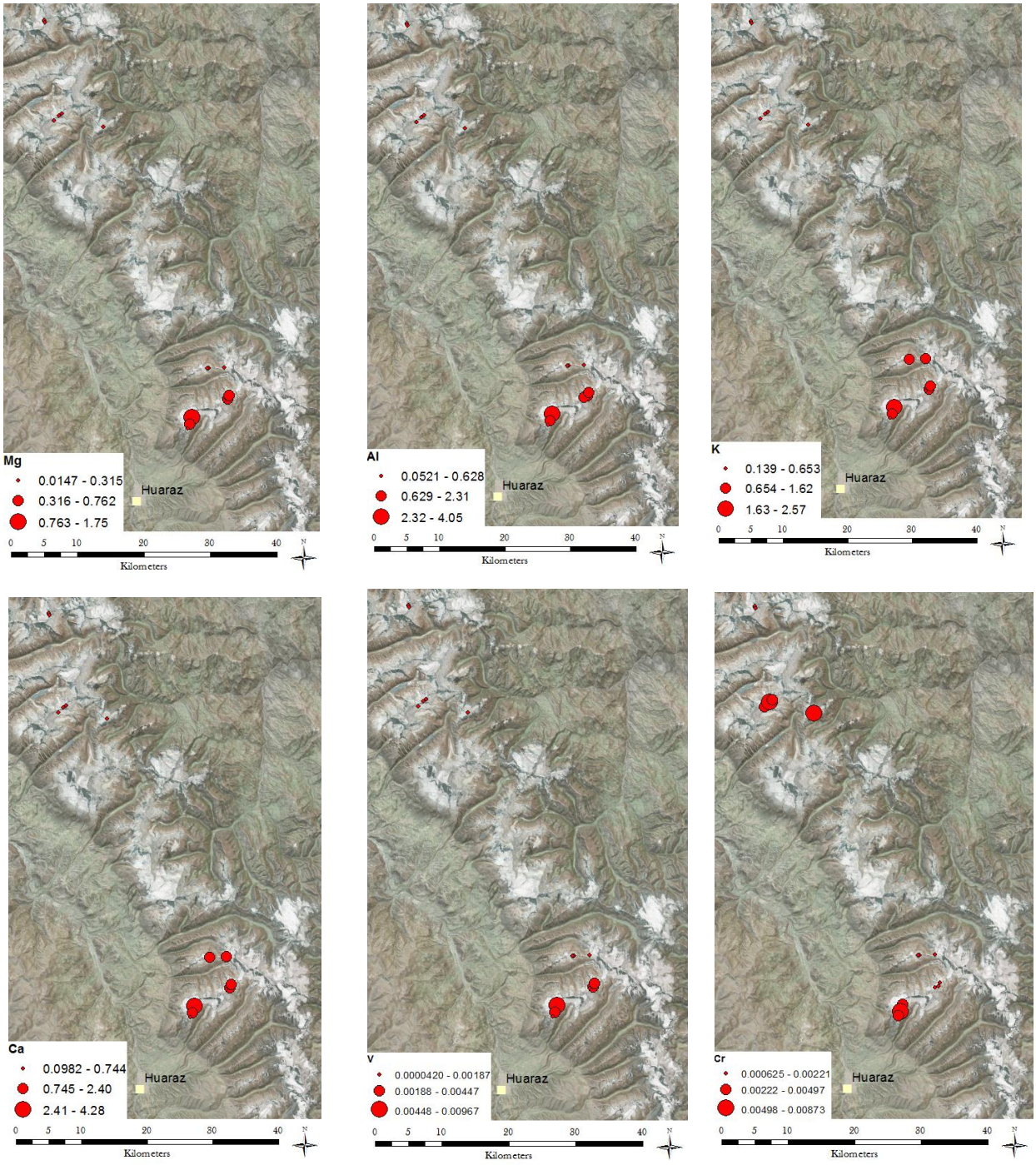

Figure S1 (continued).

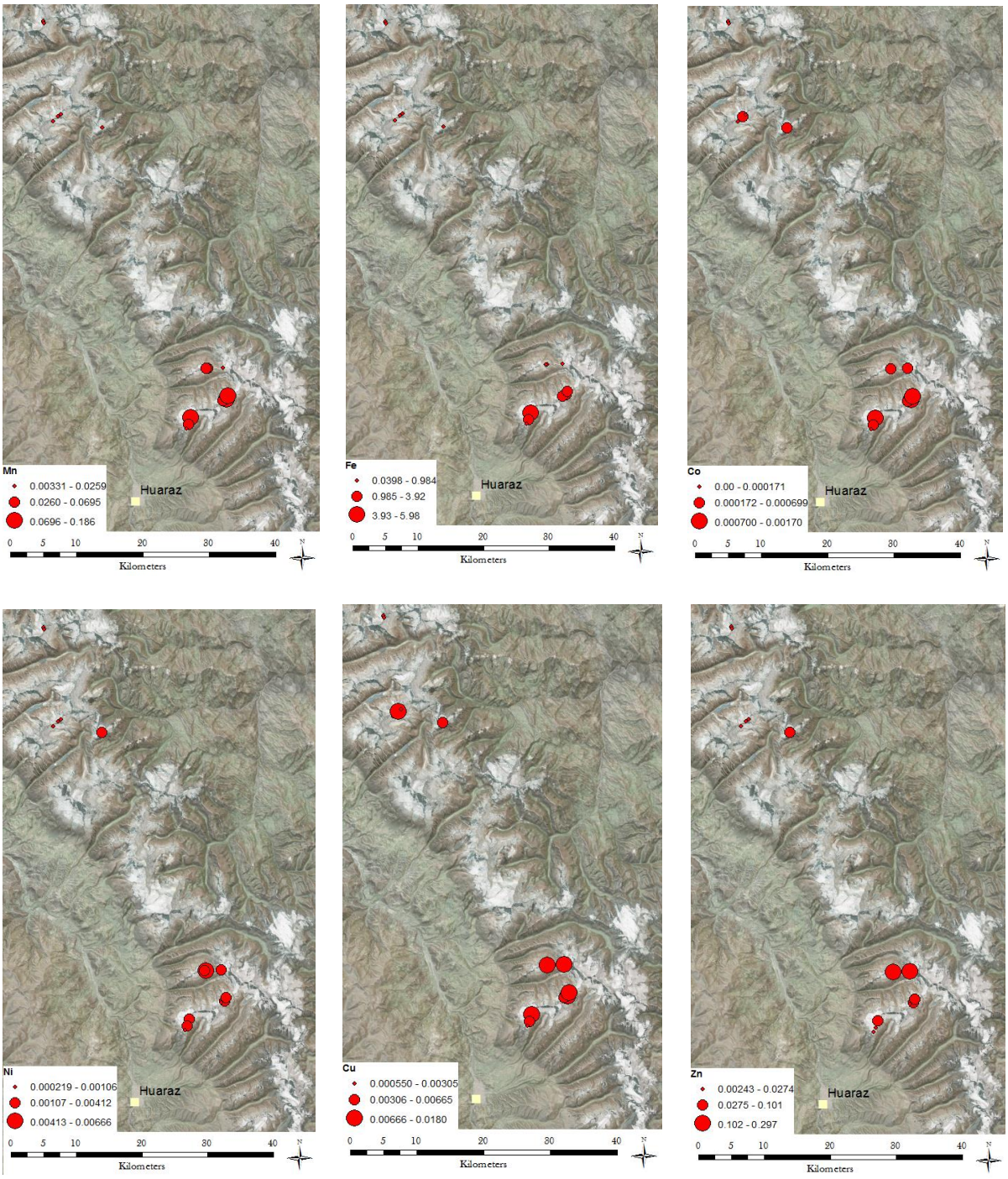

Figure S1 (continued).

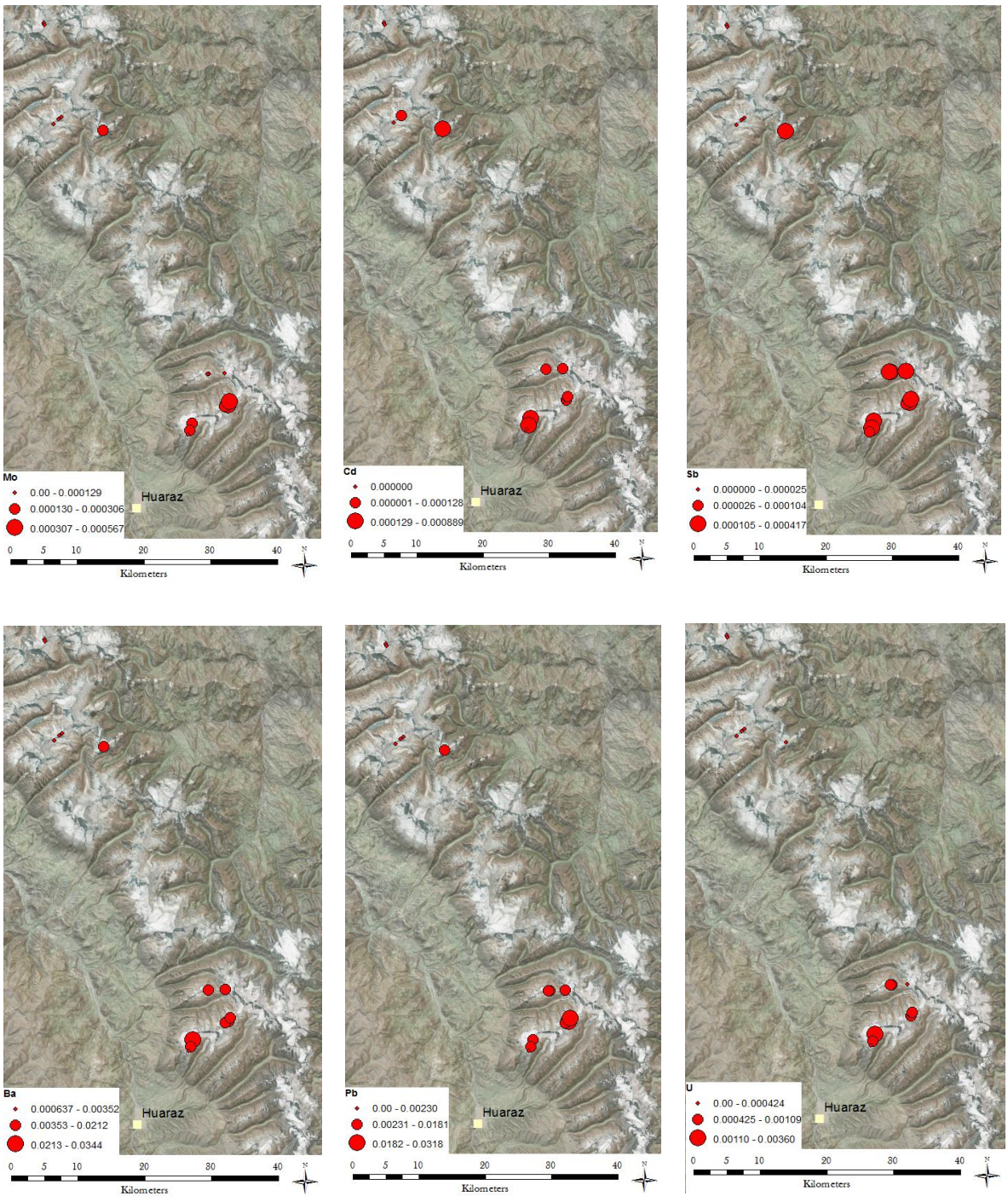

Figure S1 (continued).

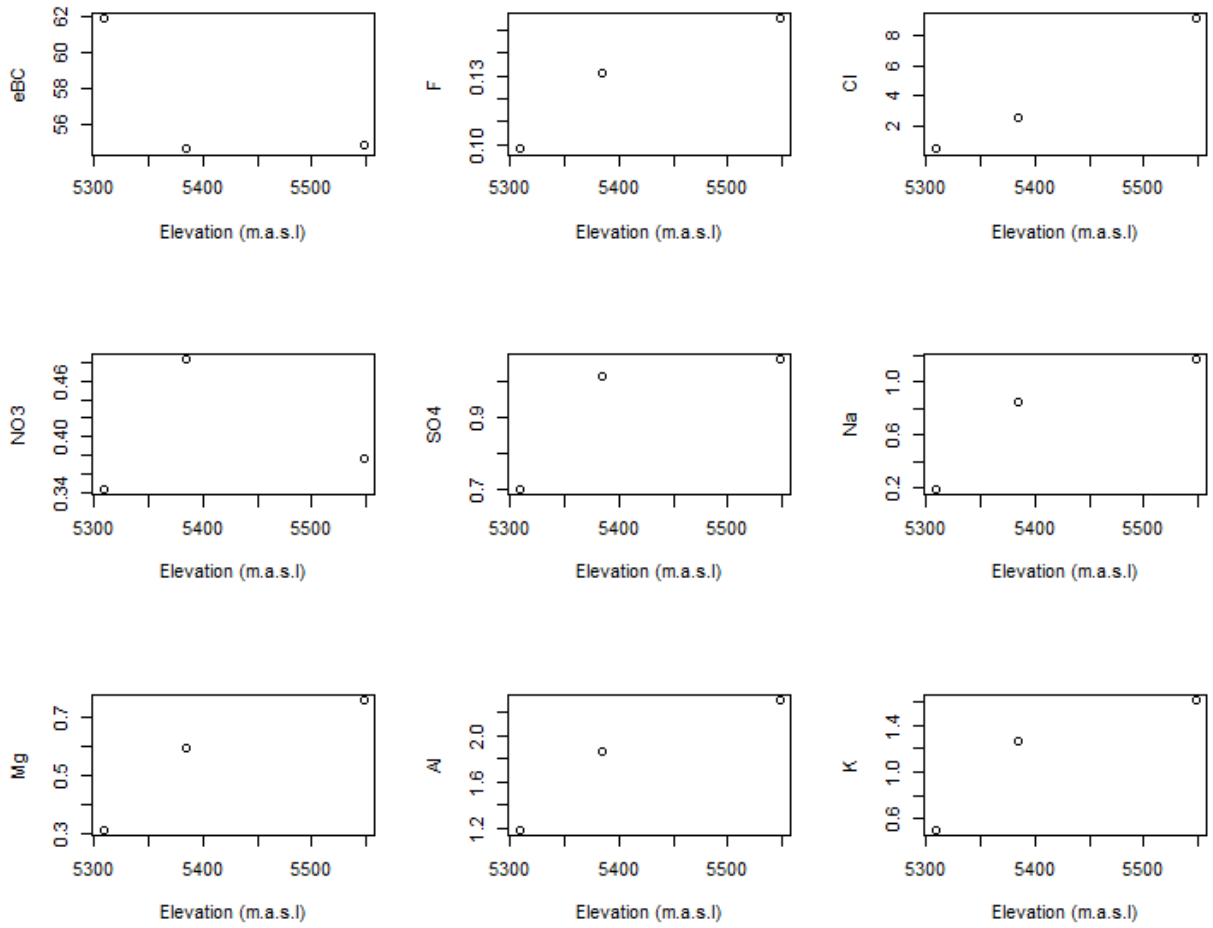

Figure S2. Scatterplot showing no significant linear relationship between elevation and any measured analytes ($p>0.05$), with the exception of Zn ($p<0.05$), for samples from Ishinca only.

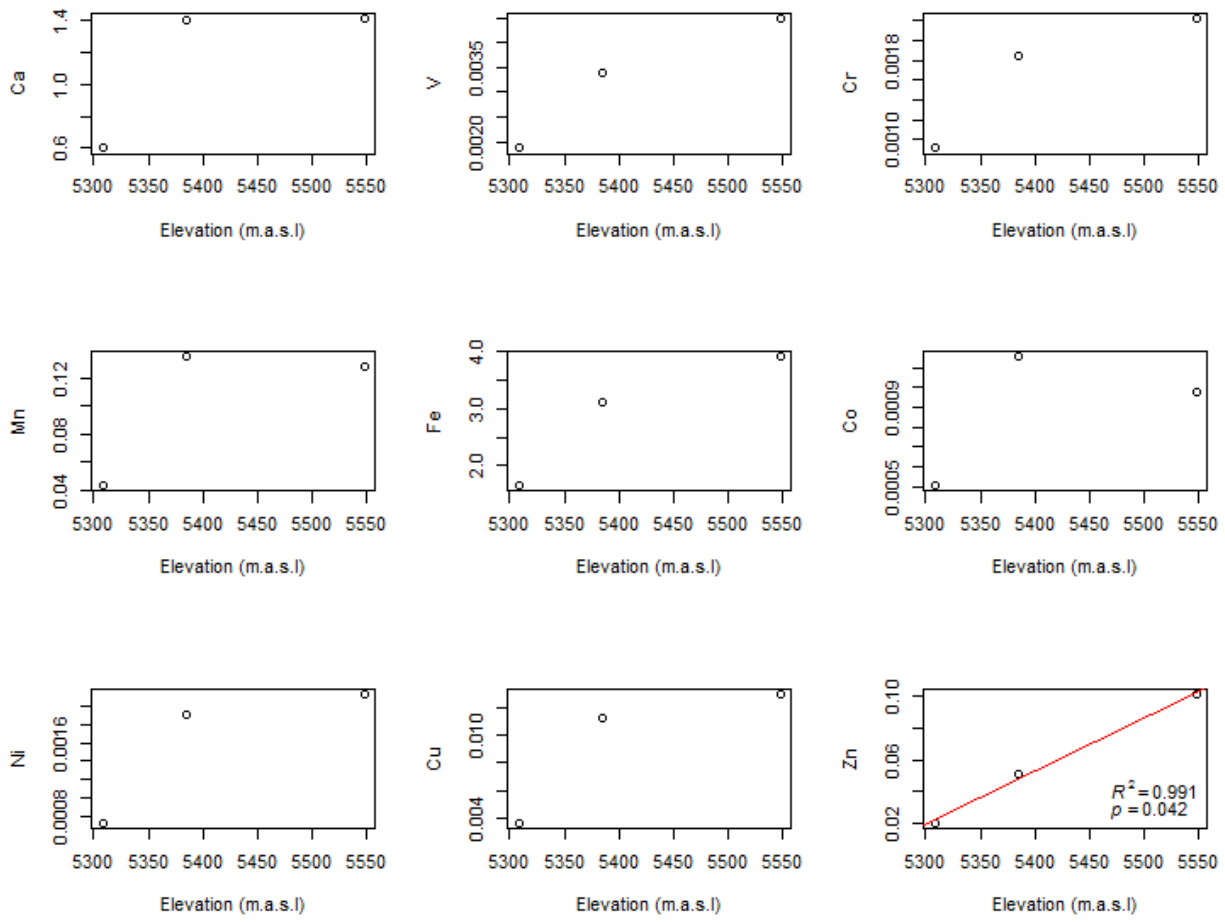

Figure S2 (continued).

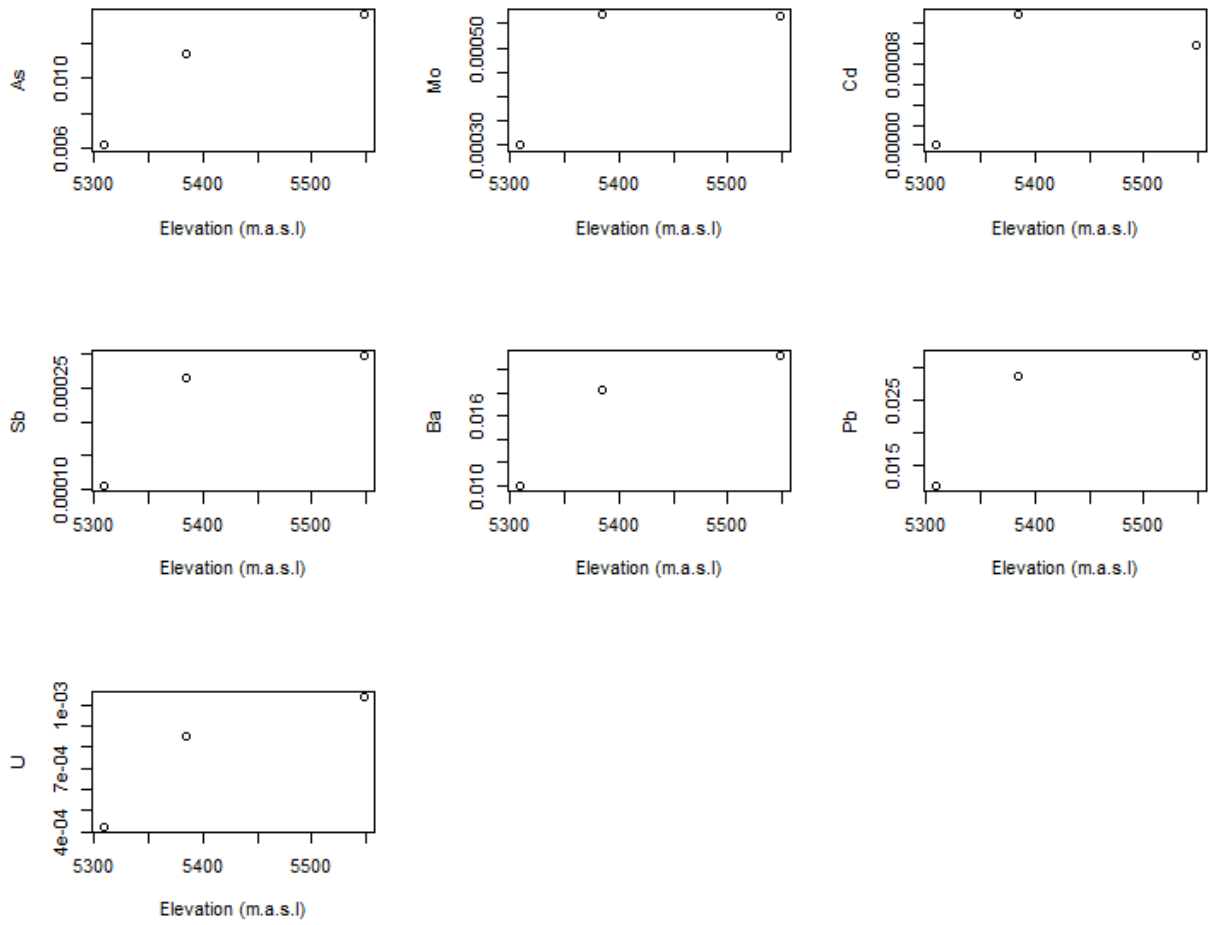

Figure S2 (continued).

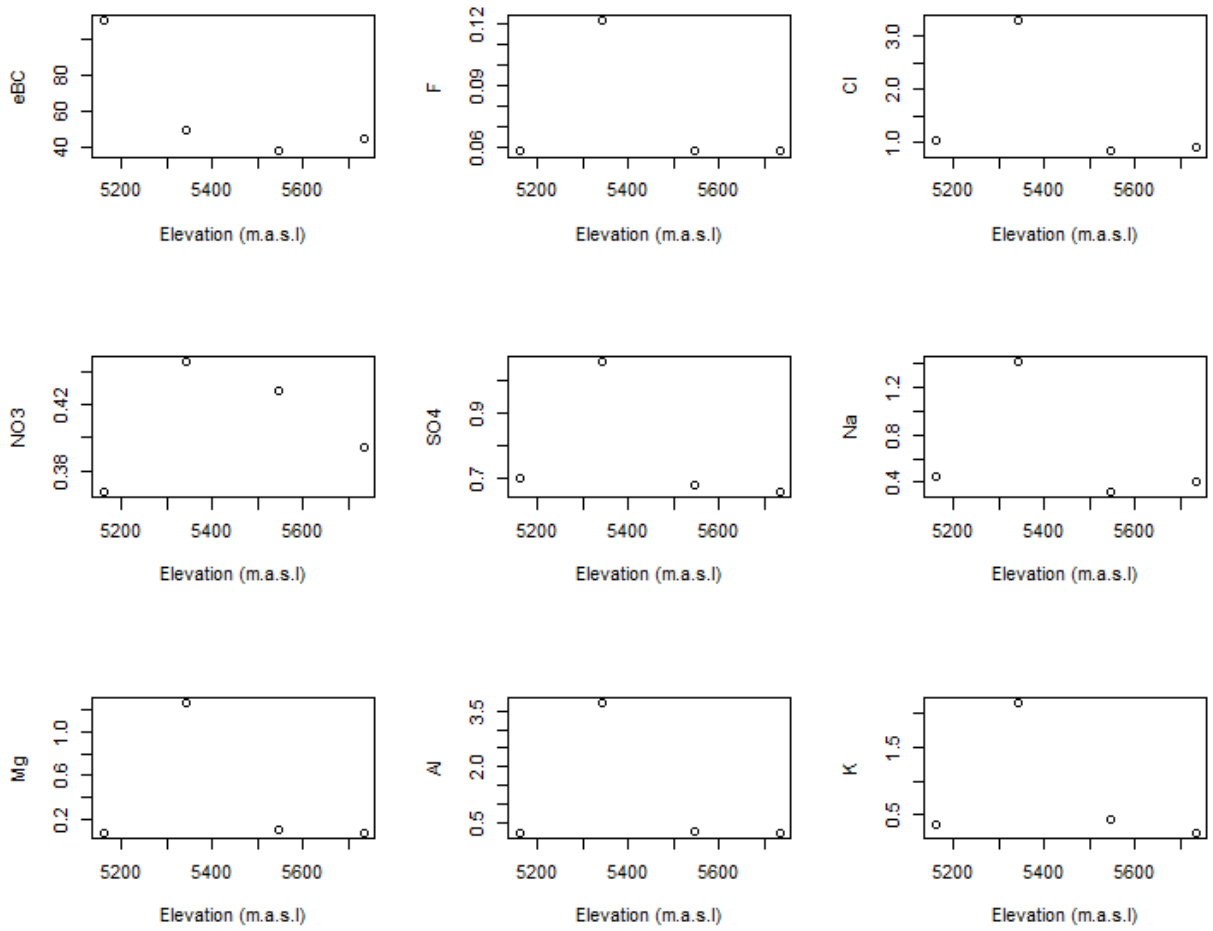

Figure S3. Scatterplot showing no significant linear relationship between elevation and any of the measured variables ($p>0.05$) for samples from Pisco only.

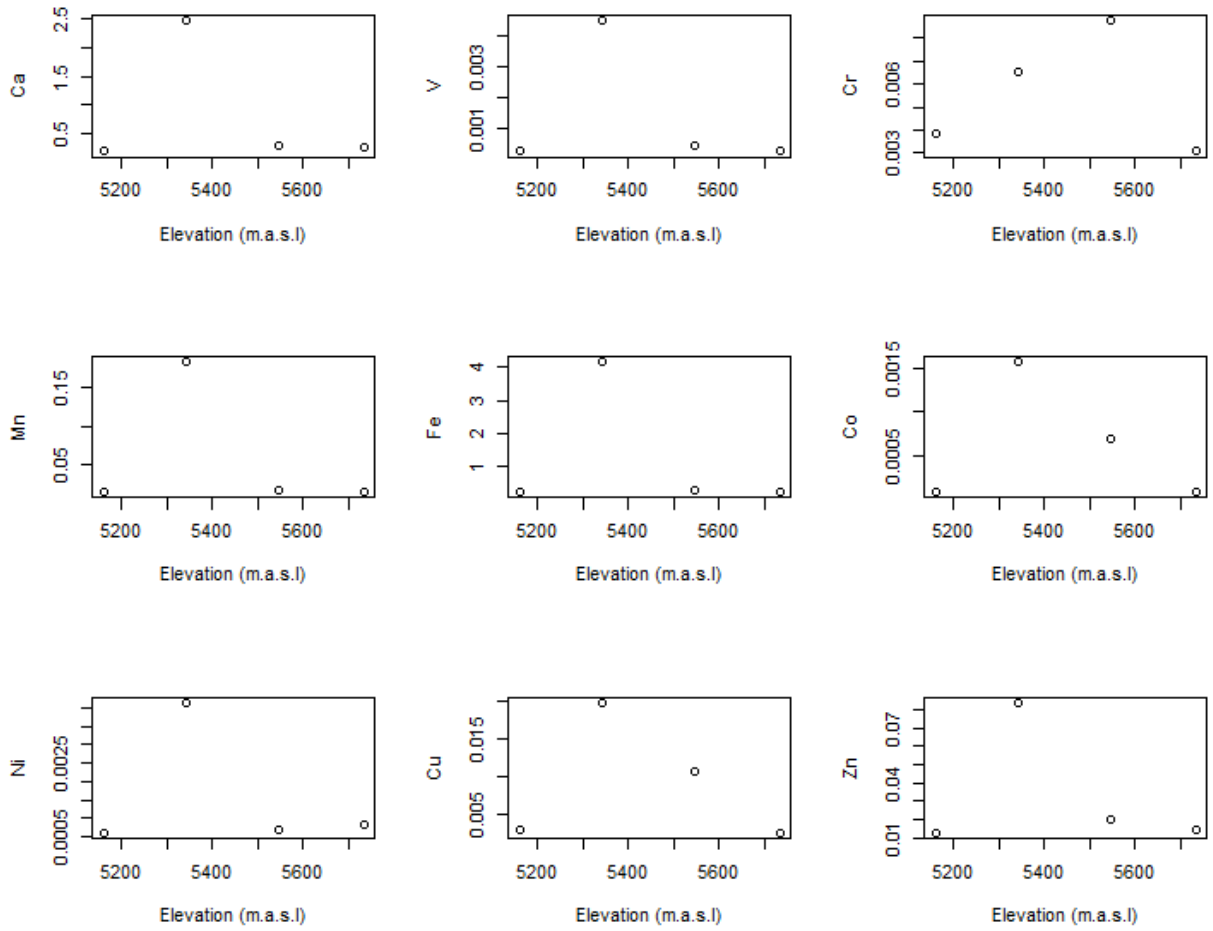

Figure S3 (continued)

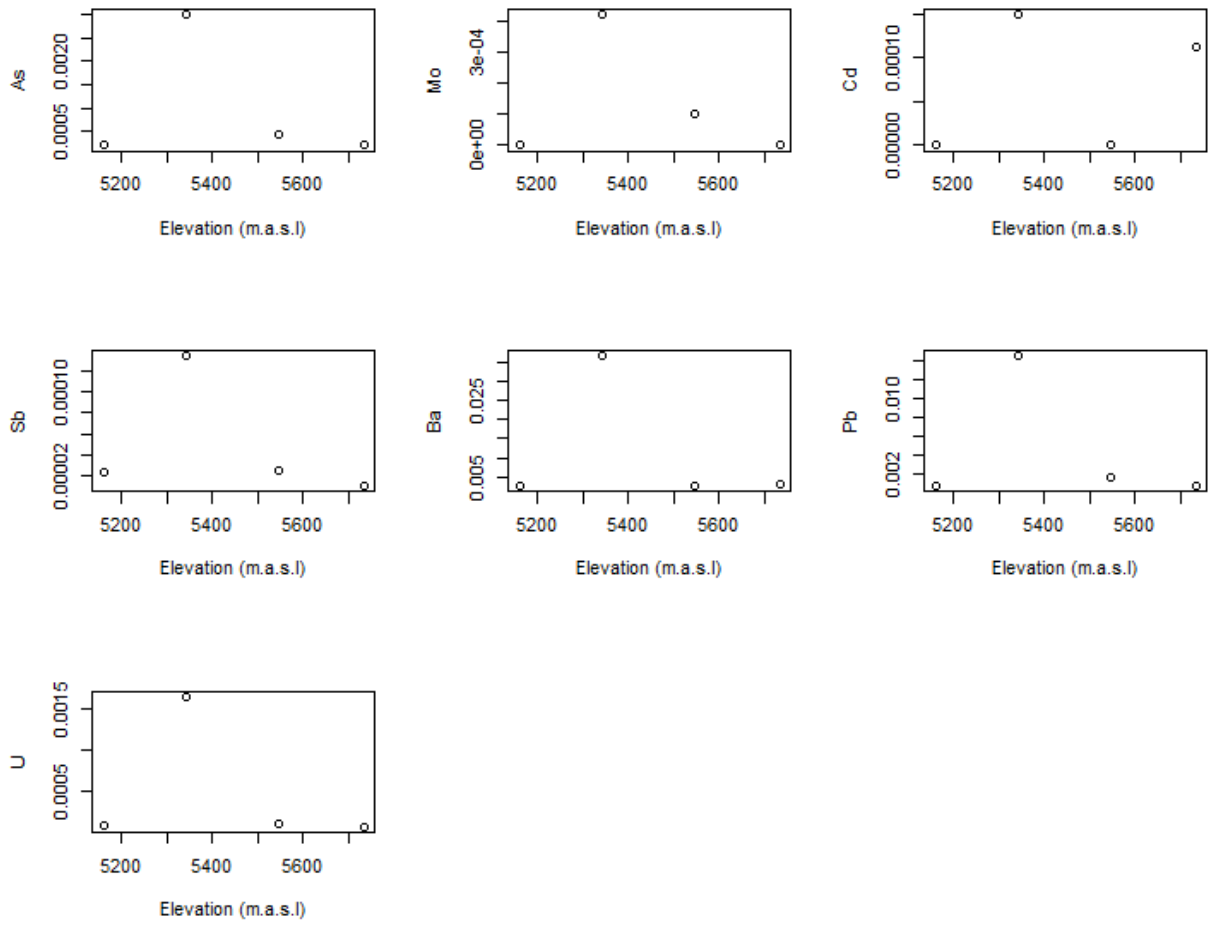

Figure S3 (continued)

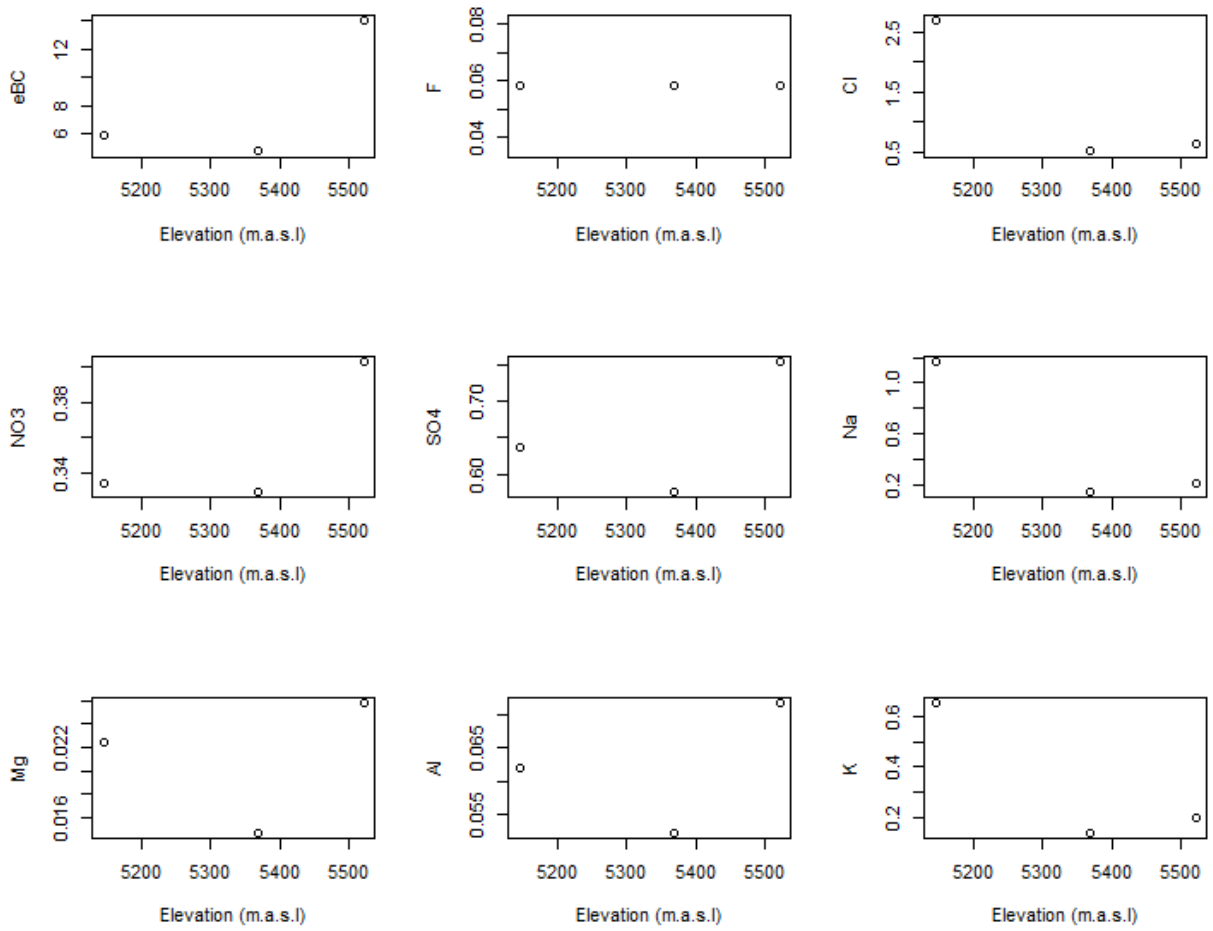

Figure S4. Scatterplot showing no significant linear relationship between elevation and any of the measured variables ($p>0.05$) for samples from Alpamayo only.

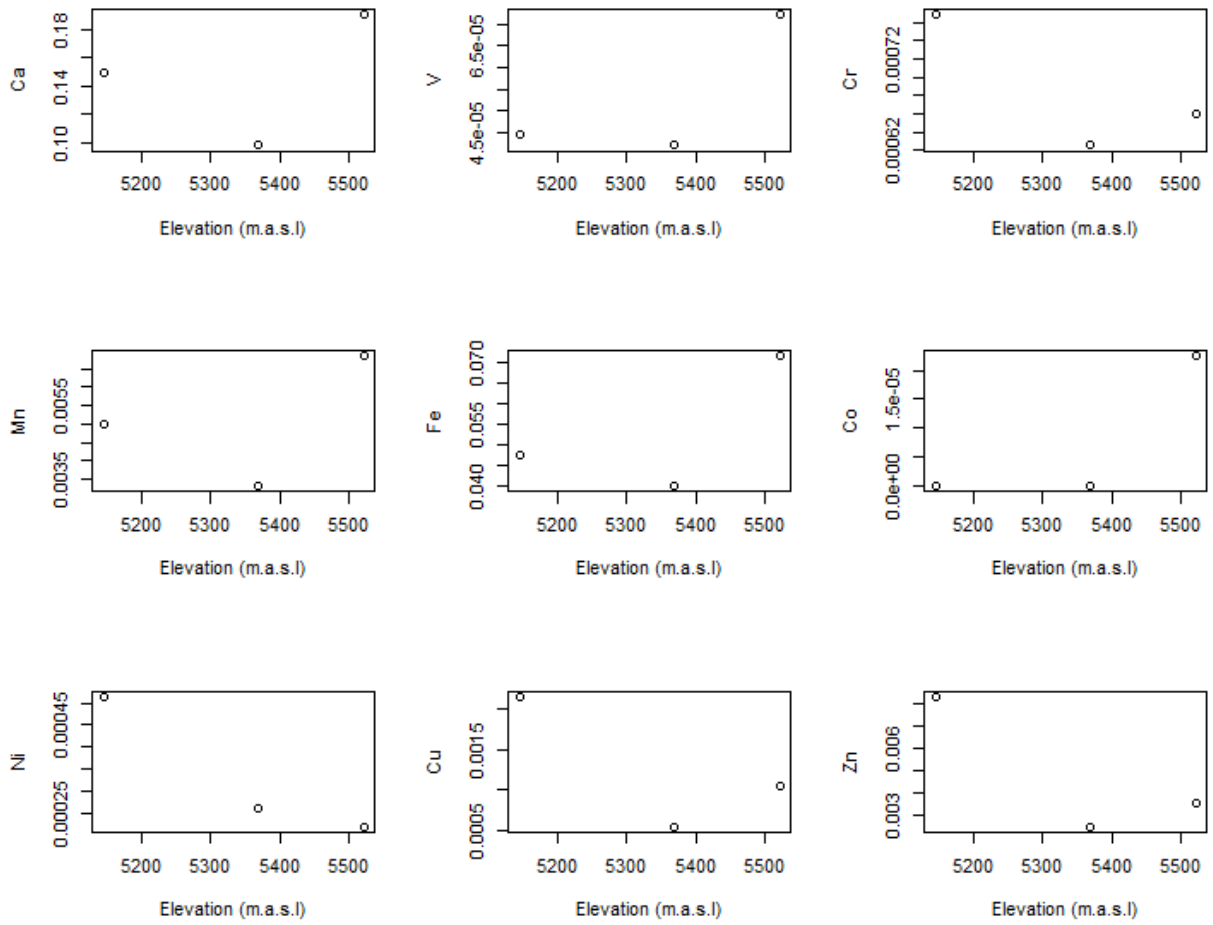

Figure S4 (continued)

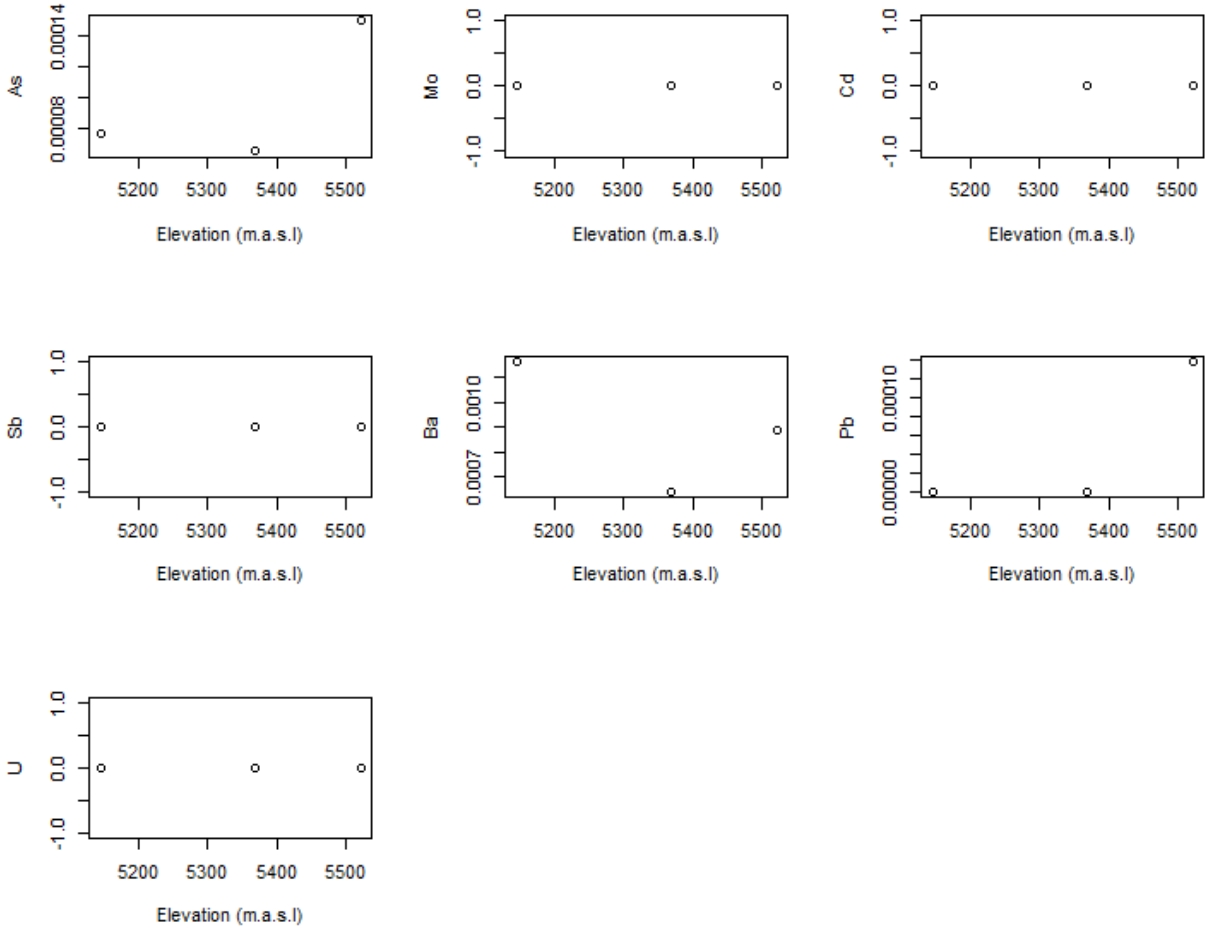

Figure S4 (continued)

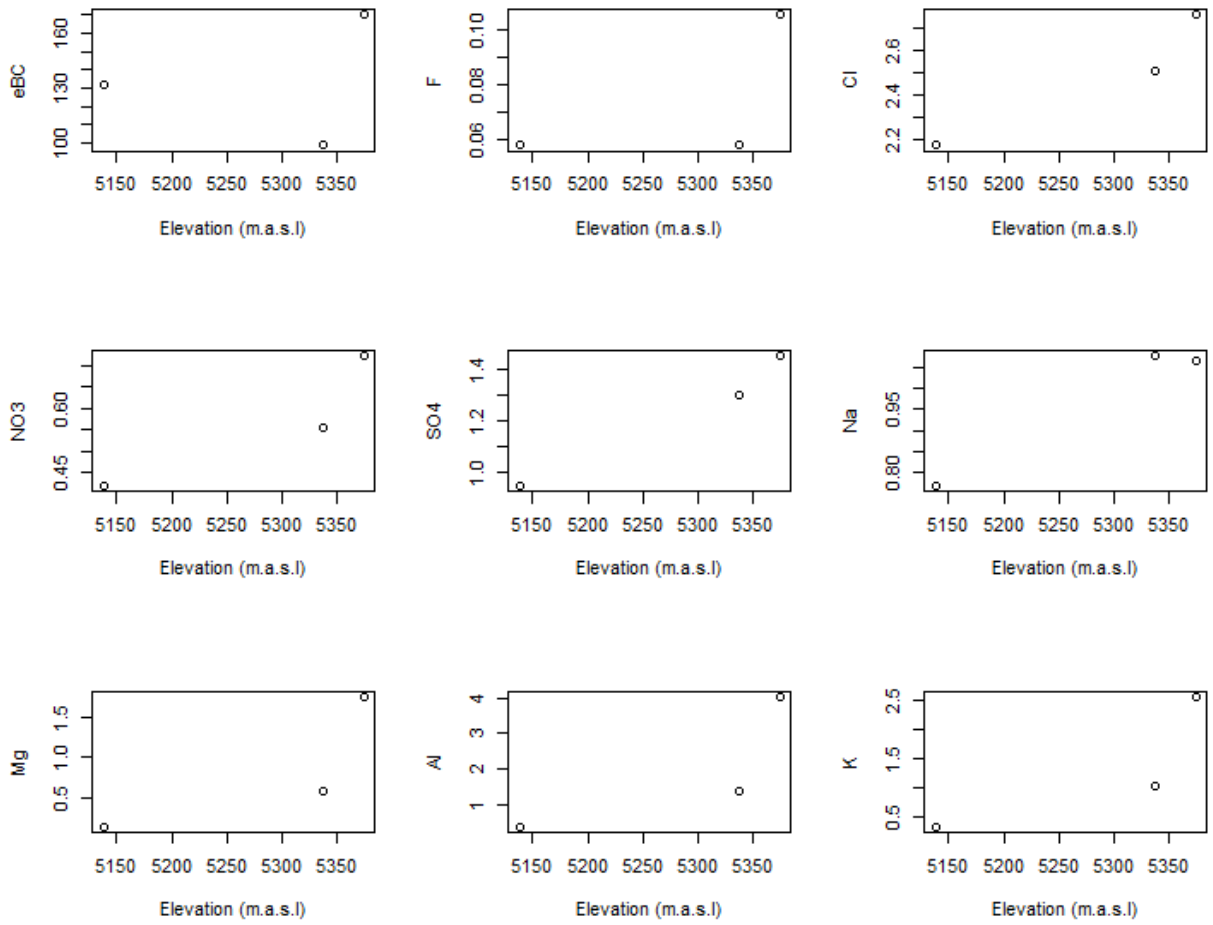

Figure S5. Scatterplot showing no significant linear relationship between elevation and any of the measured variables ($p>0.05$) for samples from Vallunaraju only.

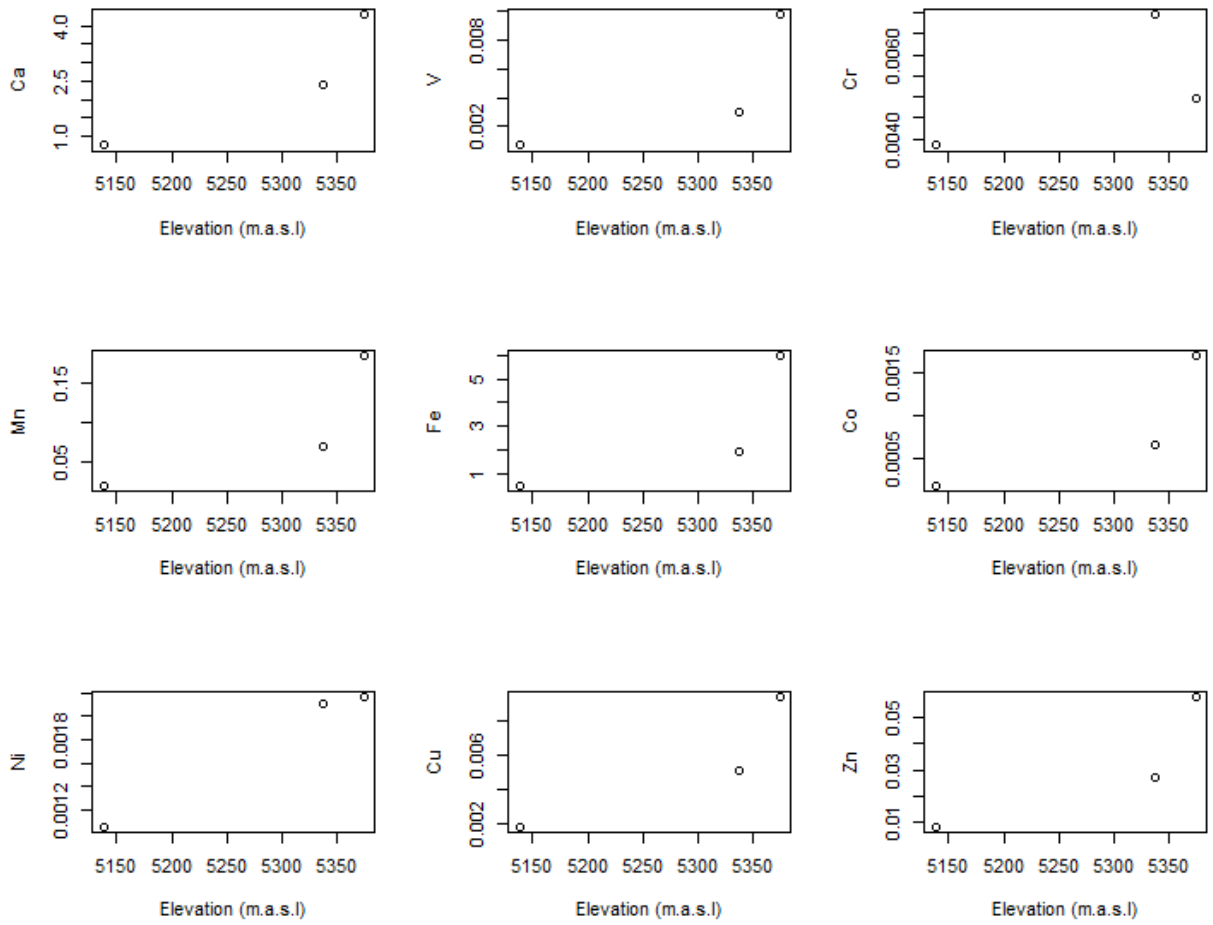

Figure S5 (continued)

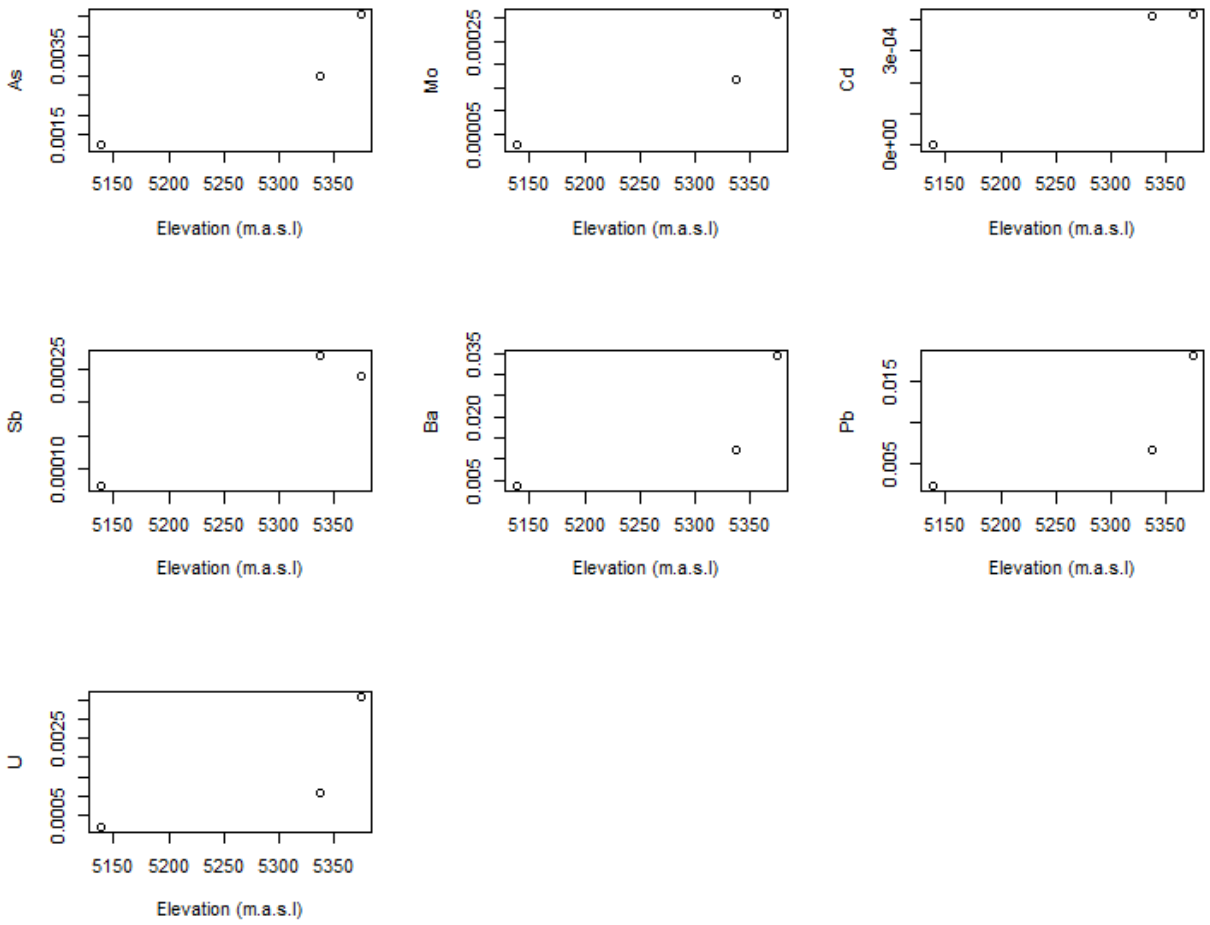

Figure S5 (continued)

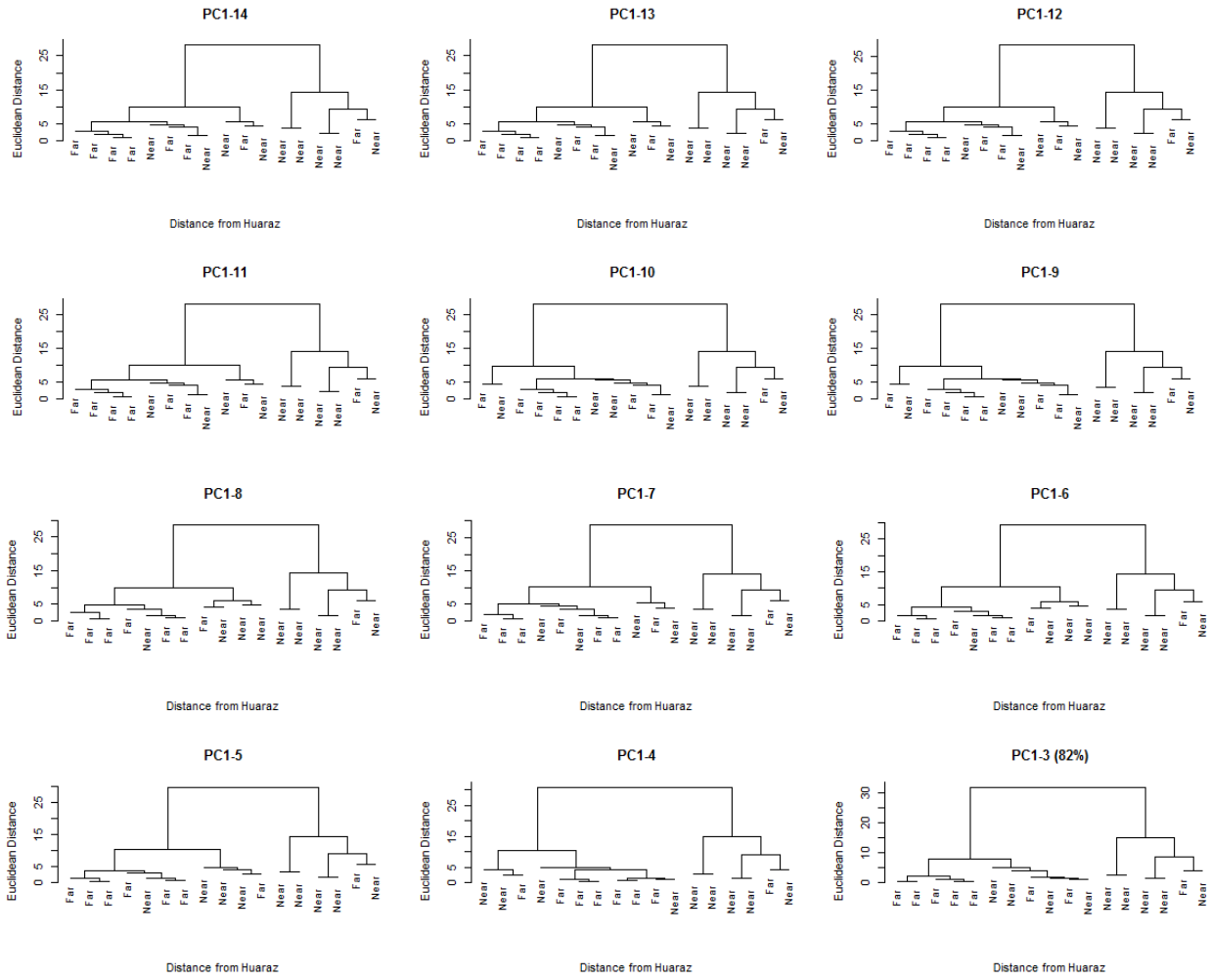

Figure S6. Hierarchical clustering on varying numbers of principal components (PCs), showing the stability of clusters and validity in using just the first three PCs.

Table S1. Correlation coefficients for effective black carbon (eBC), anions, and total metals for Combined samples (n=20). Bolded values indicate significant correlations ($p<0.05$, Kendall's τ)

	eBC	F	Cl	NO_3	SO_4	Na	Mg	Al	K	Ca	V	Cr	Mn	Fe	Co	Ni	Cu	Zn	As	Mo	Cd	Sb	Ba	Pb
F	0.26																							
Cl	0.34	**0.49**																						
NO_3	0.15	0.06	0.16																					
SO_4	**0.50**	**0.51**	**0.66**	**0.38**																				
Na	0.35	**0.42**	**0.75**	0.12	**0.47**																			
Mg	**0.40**	**0.55**	0.35	**0.40**	**0.49**	**0.43**																		
Al	**0.38**	**0.49**	0.34	**0.41**	**0.47**	**0.38**	**0.93**																	
K	0.32	**0.60**	**0.54**	0.21	**0.47**	**0.62**	**0.72**	**0.68**																
Ca	**0.50**	**0.51**	**0.46**	**0.44**	**0.65**	**0.53**	**0.81**	**0.77**	**0.68**															
V	**0.38**	**0.48**	0.31	**0.41**	**0.44**	**0.38**	**0.93**	**0.97**	**0.68**	**0.74**														
Cr	0.27	-0.03	0.04	**0.41**	0.12	0.21	0.34	**0.38**	0.27	0.32	**0.41**													
Mn	0.32	**0.51**	**0.37**	**0.50**	**0.50**	**0.38**	**0.90**	**0.88**	**0.65**	**0.77**	**0.85**	0.32												
Fe	0.35	**0.48**	0.31	**0.44**	**0.44**	0.35	**0.93**	**0.97**	**0.65**	**0.77**	**0.97**	**0.38**	**0.88**											
Co	0.27	**0.46**	0.32	**0.45**	**0.39**	**0.36**	**0.85**	**0.80**	**0.66**	**0.72**	**0.83**	**0.42**	**0.78**	**0.83**										
Ni	0.31	0.37	**0.44**	0.31	**0.46**	**0.40**	**0.47**	**0.49**	**0.40**	**0.57**	**0.46**	0.28	**0.54**	**0.49**	**0.41**									
Cu	0.25	**0.62**	**0.50**	0.22	**0.46**	**0.49**	**0.59**	**0.54**	**0.66**	**0.60**	**0.54**	0.31	**0.57**	**0.52**	**0.64**	**0.53**								
Zn	**0.41**	**0.66**	**0.57**	0.21	**0.59**	**0.47**	**0.63**	**0.59**	**0.62**	**0.68**	**0.56**	0.15	**0.62**	**0.59**	**0.57**	**0.63**	**0.78**							
As	0.35	**0.58**	0.34	0.32	**0.47**	0.24	**0.72**	**0.74**	**0.50**	**0.59**	**0.71**	0.15	**0.74**	**0.71**	**0.57**	**0.46**	**0.52**	**0.59**						
Mo	0.24	**0.66**	0.31	0.29	**0.37**	0.35	**0.79**	**0.76**	**0.63**	**0.64**	**0.76**	0.23	**0.72**	**0.75**	**0.77**	**0.40**	**0.58**	**0.61**	**0.67**					
Cd	0.30	0.32	0.25	0.31	0.30	**0.38**	**0.55**	**0.51**	**0.48**	**0.58**	**0.50**	**0.41**	**0.55**	**0.51**	**0.55**	**0.45**	**0.40**	**0.41**	0.30	**0.50**				
Sb	**0.42**	**0.52**	**0.42**	0.31	**0.54**	**0.38**	**0.62**	**0.60**	**0.44**	**0.57**	**0.57**	0.23	**0.63**	**0.57**	**0.50**	**0.56**	**0.54**	**0.68**	**0.69**	**0.56**	**0.42**			
Ba	**0.46**	**0.66**	**0.53**	0.31	**0.54**	**0.54**	**0.82**	**0.78**	**0.72**	**0.81**	**0.75**	0.31	**0.78**	**0.78**	**0.73**	**0.62**	**0.68**	**0.75**	**0.63**	**0.69**	**0.56**	**0.60**		
Pb	0.30	**0.64**	0.32	**0.36**	**0.42**	0.27	**0.82**	**0.80**	**0.54**	**0.66**	**0.78**	0.19	**0.83**	**0.80**	**0.67**	**0.49**	**0.55**	**0.63**	**0.86**	**0.80**	**0.41**	**0.65**	**0.70**	
U	**0.36**	**0.50**	**0.42**	**0.51**	**0.60**	**0.38**	**0.77**	**0.78**	**0.62**	**0.75**	**0.75**	0.35	**0.84**	**0.75**	**0.65**	**0.53**	**0.54**	**0.53**	**0.66**	**0.59**	**0.45**	**0.58**	**0.69**	**0.71**

Table S2. Correlation coefficients for effective black carbon (eBC), anions, and total metals for Near samples (n=12). Bolded values indicate significant correlations ($p<0.05$, Kendall's τ).

	eBC	**F**	**Cl**	**NO_3**	**SO_4**	**Na**	**Mg**	**Al**	**K**	**Ca**	**V**	**Cr**	**Mn**	**Fe**	**Co**	**Ni**	**Cu**	**Zn**	**As**	**Mo**	**Cd**	**Sb**	**Ba**	**Pb**
F	-0.09																							
Cl	0.28	0.49																						
NO_3	0.06	-0.26	-0.11																					
SO_4	0.44	0.32	**0.83**	0.06																				
Na	0.22	0.32	**0.72**	-0.06	**0.67**																			
Mg	0.06	0.38	0.22	0.22	0.17	0.28																		
Al	0.06	0.26	0.11	0.33	0.06	0.17	**0.89**																	
K	0.22	**0.55**	0.50	0.06	0.44	**0.56**	**0.72**	**0.61**																
Ca	0.39	0.26	0.44	0.22	**0.61**	**0.61**	**0.56**	0.44	**0.72**															
V	0.06	0.26	0.11	0.33	0.06	0.17	**0.89**	**1.00**	**0.61**	0.44														
Cr	0.17	-0.20	-0.11	**0.56**	0.06	0.17	0.22	0.33	0.17	0.33	0.33													
Mn	-0.11	0.26	0.17	0.50	0.11	0.22	**0.72**	**0.72**	**0.56**	0.39	**0.72**	0.28												
Fe	0.06	0.26	0.11	0.33	0.06	0.17	**0.89**	**1.00**	**0.61**	0.44	**1.00**	0.33	**0.72**											
Co	-0.06	0.38	0.22	0.22	0.17	0.28	**0.89**	**0.78**	**0.72**	**0.56**	**0.78**	0.11	**0.72**	**0.78**										
Ni	0.00	0.09	0.50	0.17	**0.56**	0.33	-0.17	-0.17	0.11	0.17	-0.17	-0.06	0.00	-0.17	-0.17									
Cu	0.00	**0.73**	**0.72**	-0.17	**0.56**	**0.56**	0.28	0.17	**0.56**	0.39	0.17	-0.17	0.33	0.17	0.28	0.33								
Zn	0.22	**0.61**	**0.83**	-0.17	**0.67**	**0.56**	0.28	0.17	**0.56**	0.39	0.17	-0.28	0.22	0.17	0.28	0.44	**0.78**							
As	-0.33	**0.55**	0.06	-0.06	-0.11	-0.11	0.50	0.50	0.22	0.06	0.50	-0.17	0.44	0.50	0.39	-0.11	0.33	0.22						
Mo	-0.22	**0.55**	0.17	0.06	0.00	0.22	**0.72**	**0.61**	**0.56**	0.39	**0.61**	-0.06	**0.56**	**0.61**	**0.83**	-0.33	0.33	0.22	**0.56**					
Cd	0.15	0.33	0.26	0.44	0.44	0.44	**0.61**	0.49	**0.67**	**0.78**	0.49	0.38	**0.67**	0.49	**0.73**	0.03	0.32	0.26	0.15	**0.55**				
Sb	-0.06	0.44	0.44	0.00	0.39	0.39	0.22	0.11	0.17	0.11	0.11	0.00	0.28	0.11	0.11	0.28	0.50	0.50	0.28	0.17	0.26			
Ba	0.22	**0.67**	0.50	0.06	0.44	0.44	**0.72**	**0.61**	**0.89**	**0.61**	**0.61**	0.17	**0.56**	**0.61**	**0.72**	0.11	**0.56**	**0.56**	0.33	**0.56**	**0.67**	0.28		
Pb	-0.22	**0.55**	0.06	0.06	-0.11	0.00	**0.61**	**0.61**	0.33	0.17	**0.61**	-0.06	**0.56**	**0.61**	0.50	-0.11	0.33	0.22	**0.89**	**0.67**	0.26	0.28	0.44	
U	0.00	0.15	0.06	**0.61**	0.22	0.22	**0.61**	**0.61**	0.44	0.50	**0.61**	0.50	**0.78**	**0.61**	0.50	0.11	0.22	0.11	0.33	0.33	**0.67**	0.28	0.44	0.44

Table S3. Correlation coefficients for effective black carbon (eBC), anions, and total metals for Far samples (n=8). Bolded values indicate significant correlations ($p<0.05$, Kendall's τ).

	eBC	**F**	**Cl**	**NO_3**	**SO_4**	**Na**	**Mg**	**Al**	**K**	**Ca**	**V**	**Cr**	**Mn**	**Fe**	**Co**	**Ni**	**Cu**	**Zn**	**As**	**Mo**	**Cd**	**Sb**	**Ba**	**Pb**
F	0.21																							
Cl	0.36	0.50																						
NO_3	0.21	0.50	0.14																					
SO_4	0.29	0.50	0.36	**0.64**																				
Na	0.43	0.50	**0.79**	0.07	0.14																			
Mg	0.57	0.50	0.21	**0.64**	0.29	0.43																		
Al	**0.64**	0.50	0.29	0.57	0.36	0.50	**0.93**																	
K	0.21	0.50	**0.71**	0.29	0.21	**0.79**	0.50	0.57																
Ca	0.50	0.50	0.14	**0.71**	0.36	0.36	**0.93**	**0.86**	0.43															
V	**0.64**	0.50	0.29	0.57	0.36	0.50	**0.93**	**1.00**	0.57	**0.86**														
Cr	0.43	0.36	0.36	0.50	0.29	0.43	**0.71**	**0.79**	**0.64**	**0.64**	**0.79**													
Mn	0.57	0.50	0.21	**0.64**	0.29	0.43	**1.0**	**0.93**	0.50	**0.93**	**0.93**	**0.71**												
Fe	0.57	0.50	0.21	**0.64**	0.29	0.43	**1.0**	**0.93**	0.50	**0.93**	**0.93**	**0.71**	**1.0**											
Co	0.47	0.51	0.26	**0.69**	0.33	0.33	**0.91**	**0.84**	0.55	**0.84**	**0.84**	**0.76**	**0.91**	**0.91**										
Ni	0.50	0.50	0.29	0.43	0.07	0.50	**0.79**	**0.71**	0.43	**0.71**	**0.71**	**0.64**	**0.79**	**0.79**	**0.69**									
Cu	0.50	0.50	0.43	0.57	0.36	0.50	**0.79**	**0.86**	**0.71**	**0.71**	**0.86**	**0.93**	**0.79**	**0.79**	**0.84**	**0.71**								
Zn	0.50	0.50	0.29	0.57	0.21	0.50	**0.93**	**0.86**	0.57	**0.86**	**0.86**	**0.79**	**0.93**	**0.93**	**0.84**	**0.86**	**0.86**							
As	**0.64**	0.50	0.29	0.57	0.36	0.50	**0.93**	**1.00**	0.57	**0.86**	**1.00**	**0.79**	**0.93**	**0.93**	**0.84**	**0.71**	**0.86**	**0.86**						
Mo	0.36	0.62	0.18	0.54	0.18	0.45	**0.80**	**0.80**	0.54	**0.80**	**0.80**	**0.62**	**0.80**	**0.80**	**0.73**	**0.71**	**0.71**	**0.80**	**0.80**					
Cd	0.54	0.45	0.18	0.27	0.00	0.45	**0.62**	0.54	0.27	**0.62**	0.54	0.36	**0.62**	**0.62**	0.54	**0.71**	0.45	**0.62**	0.54	0.56				
Sb	**0.64**	0.38	0.19	0.42	0.19	0.42	**0.79**	**0.87**	0.49	**0.72**	**0.87**	**0.72**	**0.79**	**0.79**	**0.73**	**0.72**	**0.79**	**0.79**	**0.87**	**0.75**	**0.66**			
Ba	**0.64**	0.50	0.43	0.43	0.21	**0.64**	**0.79**	**0.71**	0.43	**0.71**	**0.71**	**0.64**	**0.79**	**0.79**	**0.69**	**0.86**	**0.71**	**0.86**	**0.71**	**0.62**	**0.71**	**0.64**		
Pb	0.55	0.51	0.18	**0.62**	0.26	0.40	**0.98**	**0.91**	0.47	**0.91**	**0.91**	**0.69**	**0.98**	**0.98**	**0.93**	**0.76**	**0.76**	**0.91**	**0.91**	**0.82**	**0.64**	**0.81**	**0.76**	
U	0.49	0.53	0.49	0.57	0.49	0.27	**0.64**	**0.72**	0.49	0.57	**0.72**	**0.72**	**0.64**	**0.64**	**0.73**	0.57	**0.79**	**0.64**	**0.72**	0.57	0.28	**0.68**	0.49	**0.65**

Table S4. Correlation coefficients for effective black carbon (eBC), anions, and total metals for Combined (n=20), Near (n=12), and Far samples (n=8). Bolded values indicate significant correlations ($p<0.05$, Kendall's τ).

	Combined	Near	Far
eBC	-0.26	-0.21	0.071
F	0.009	0.34	-0.07
Cl	-0.19	0.071	-0.14
NO_3	0.059	0	0.43
SO_4	-0.24	-0.07	0.071
Na	-0.15	0.14	-0.29
Mg	0.10	**0.86**	0.21
Al	0.088	**0.86**	0.14
K	0	0.50	-0.14
Ca	-0.03	0.29	0.29
V	0.12	**0.86**	0.14
Cr	0.15	0.21	0.29
Mn	0	0.50	0.21
Fe	0.12	**0.86**	0.21
Co	0.20	**0.71**	0.33
Ni	-0.22	-0.42	0.21
Cu	0.074	0.21	0.21
Zn	-0.06	0.14	0.14
As	-0.06	0.50	0.14
Mo	0.12	**0.64**	0.089
Cd	0.22	0.34	0.27
Sb	-0.07	0.29	0.19
Ba	-0.02	0.50	0.14
Pb	0.081	0.50	0.26
U	-0.07	0.36	0.19

Table S5. Median analyte concentrations with sample P2 (Table 1) removed. Bolded names and values indicate a significant difference ($p<0.05$, Kruskal-Wallis).

	Near	Far
eBC	**99**	**37**
Cl	**2.6**	**0.82**
Fe	**1.6**	**0.23**
Ca	**1.4**	**0.19**
Al	**1.2**	**0.21**
SO_4	**1.1**	**0.65**
K	**1**	**0.35**
Na	0.92	0.4
NO_3	0.42	0.38
Mg	**0.31**	**0.071**
F	**0.11**	**0.058**
Mn	**0.052**	**0.013**
Zn	**0.051**	**0.013**
Ba	**0.013**	**0.0026**
Pb	**0.01**	**7.50E-04**
Cu	0.0094	0.0026
As	**0.0045**	**0.0002**
Ni	**0.0021**	**0.0006**
Cr	0.0019	0.0031
V	**0.0019**	**2.42E-04**
U	**0.00065**	**6.60E-05**
Co	**0.00051**	**8.16E-05**
Sb	**0.00025**	**1.00E-05**
Mo	**0.00017**	**0**
Cd	0.000096	0